Jürgen König

Fire exposed simply supported wooden I-joists in floor assemblies

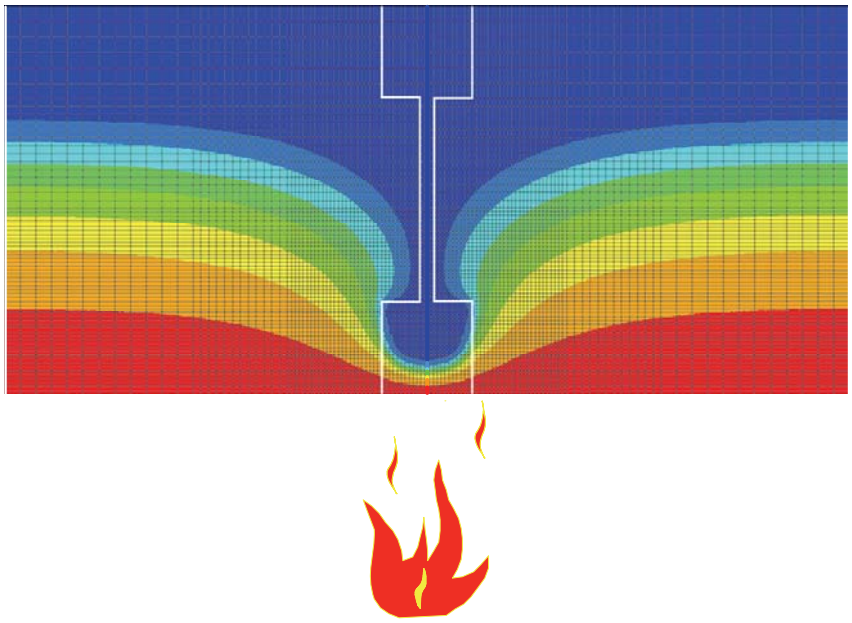

SP Swedish National Testing and Research Institute

SP Wood Technology
SP REPORT 2006:44

Jürgen König
SP Trätek/Wood Technology

Fire exposed simply supported wooden I-joists in floor assemblies

Abstract

A numerical study was conducted with the objective of determining cross-sectional and strength and stiffness properties of I-shaped joists subjected to charring under ISO 834 standard fire exposure. Model parameters were derived in terms of Eurocode 5 (EN 1995-1-2) for I-joists in bending where the tension flange is on the fire exposed side of the joist. The I-joists were assumed to be integrated in floor assemblies consisting of joists, linings made of gypsum plasterboard or wood-based panels, cavities completely filled with batt-type rock or glass fibre insulation, and a decking. Heat transfer and structural analyses were performed to study the effect of lining performance on charring and the reduction of strength properties of the I-joists.

Key words: assemblies, design, fire, floors, I-joists, modelling, resistance, timber structures

SP Sveriges Provnings- och Forskningsinstitut
SP Rapport 2006:44
ISBN 91-85533-32-7
ISSN 0284-5172
Stockholm 2006

SP Swedish National Testing and Research Institute
SP Report 2006:44
Postal address:
Box 5609, Sweden
SE-114 86 Stockholm, Sweden
Telephone: +46 8 762 1800
Telefax: +46 8 762 1801
E-mail: info@sp.se

Contents

Preface

Without the persistent enthusiastic request by Erling Johansson at Swelite AB, Sweden, to develop a design model for wooden I-joists, this project would never have been started. Further prerequisites of the project were the financial support of Swelite AB and the two other Nordic producers of wooden I-joists Finnforest (Finland) and Forestia (Norway) as well as the Nordic Innovation Centre (NICe) and the Swedish Agency for Innovation Systems (Vinnova).

Another prerequisite was the contribution by Bo Källsner who modified and improved an earlier version of his program CSTFire. Bo also acted as a valuable and patient sounding board whenever problems had to be ventilated. Per Berg modified CSTFire in order to communicate with the software SAFIR for thermal analyses, provided by University of Liège.

Summary

A numerical study was conducted with the objective of determining cross-sectional and strength and stiffness properties of I-shaped joists subjected to charring under ISO 834 standard fire exposure. The outcome of this work should be design parameters in terms of Eurocode 5 (EN 1995-1-2) for I-joists in bending where the tension flange is on the fire exposed side of the joist; these are the time of start of charring, charring depths and modification factors for strength. The I-joists are assumed to be integrated in floor assemblies consisting of joists, linings made of gypsum plasterboard or wood-based panels, cavities completely filled with batt-type rock or glass fibre insulation, and a decking. Heat transfer analyses were performed using SAFIR. This software permits us to study the effect of the lining falling off at specified times that are known from full-scale testing or using the criterion of insufficient penetration length of fasteners into unburnt wood. For the determination of the notional charring depth in the flange and the modification factors of the whole cross-section, a computer program CSTFire, written as a Visual Basic macro embedded in Excel, was developed, using the temperature output from the heat transfer calculations and relative strength and stiffness values given by EN 1995-1-2, i.e. compressive strength, tensile strength and moduli of elasticity in compression and tension. The notional charring depth is determined such that the notional residual cross-section of the flange remains rectangular and the section modulus of the I-section is unchanged. The effect of various parameters on the notional charring rate is shown, such as charring phases (i.e. a distinction is made regarding whether the I-section is initially unprotected, protected by a lining, or unprotected after failure of the lining), flange dimensions and depth of cross-section. Modification factors for bending and shear strength are shown as functions of the notional charring depth for different charring phases. In order to simplify these relationships, simple expressions are given for increased user-friendliness and code specification. The effect of the state of stress on the fire-exposed side is demonstrated, however, it remains unclear to what extent bending moment resistance at intermediate supports can be utilized.

1 Introduction

Wooden I-shaped joists and studs, consisting of flanges made of solid timber or LVL and a web made of wood-based panels (such as particle board, fibreboard or OSB), are increasingly used in timber frame construction. While design models for fire exposed timber frame construction with solid timber joists and studs are available [1][2], there is still a need to develop corresponding rules for timber frame assemblies with I-shaped joists and studs. For the time being, fire resistance classification is normally done by fire testing of floor and wall assemblies.

The constructions dealt with in this report consist of wooden I-joists with a lining, a decking (generally termed fire protective claddings) and cavities that are completely filled with batt-type rock or glass fibre insulation. The lining may be fixed to the I-joists or to resilient channels or battens in perpendicular direction to the I-joists. This report mainly deals with I-joists in bending where the tension flange is on the fire exposed side of the floor assembly; the situation at intermediate supports of floors with several spans is studied.

The normal design procedure of timber members exposed to fire consists of several steps:
- Determination of action effects (internal forces and moments);
- Determination of the residual cross-section of the member taking into account the effect of fire protective claddings (thermal analysis) on the charring depth;
- Determination of the degradation of strength and stiffness properties, e.g. by modification factors or the use of an effective residual cross-section where applicable;
- Calculation of the mechanical resistance of the member.

The goal of the study presented here was to derive simple, easy-to-use expressions for the following parameters:
- Time of start of charring;
- Charring rates;
- Modification factors for the reduction bending and shear strength.

Since failure times of fire protective claddings are not known for all types of claddings used in practice, the design model should also be applicable where failure times of fire protective claddings must be determined by testing.

For application of the results from the thermal and mechanical analyses in a simplified design model, the following goals were set up:
- The design model should be easy to use and available to all designers; it was not our purpose to create a design tool that could be felt as a “black box”;
- Charring and strength parameters should be given as linear expressions;
- The charring model should be consistent with testing and be modified where other species or engineered wood with different charring performance are used.

2 Model for the design of I-joists

2.1 General

The design model developed for I-joists follows the method and terminology and describes relevant parameters given in EN 1995-1-2 [1]. Charring rates and charring depths are expressed as notional values in order to simplify design work. Different charring phases are taken into account with respect to the effect of claddings and their failure, see Figure 2.1 and 2.2. The degradation of strength due to elevated temperature is taken into account by multiplying the bending and shear strength values at ambient temperature by modification factors.

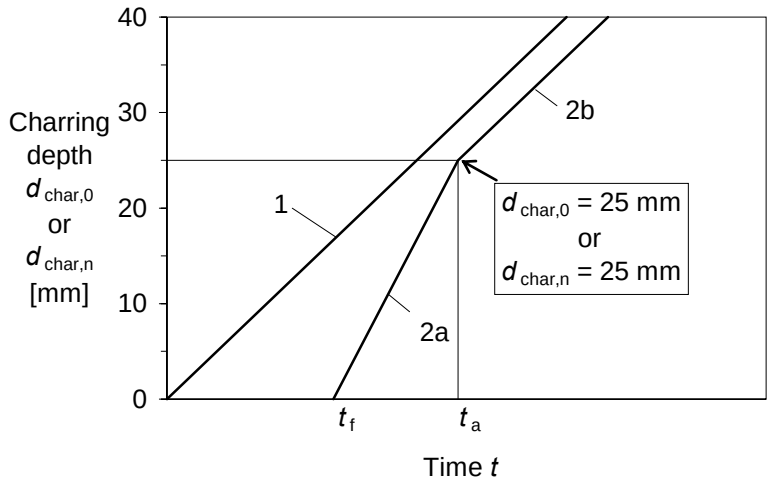

Figure 2.1: General description of charring phases for one-dimensional charring according to EN 1995-1-2 [1] when failure of the cladding occurs at the time of start of charring (lines 2a and 2b). Line 1 is for initially unprotected timber.

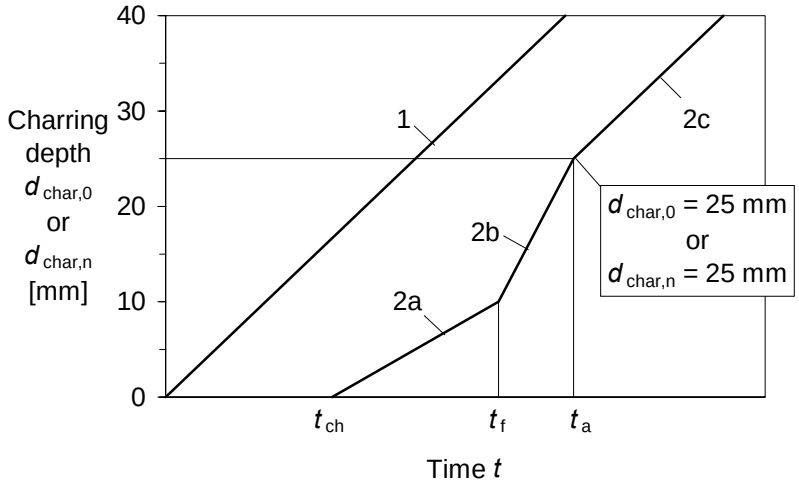

Figure 2.2: General description of charring phases for one-dimensional charring according to EN 1995-1-2 when the failure time of the cladding is greater than the time of start of charring.

With respect to the degree of protection provided by the cladding, three different charring phases are defined [3]:

- Charring phase 1 for initially unprotected timber surfaces (line 1 of Figure 2.1 and 2.2). For timber frame assemblies with I-joists this charring phase won't exist in practice.
- Charring phase 2 for the phase between start of charring of the timber member behind the cladding until failure of the cladding (line 2a of Figure 2.2).
- Charring phase 3 for the phase after failure of the cladding (line 2a and 2b of Figure 2.1 and lines 2b and 2c of Figure 2.2).

For timber floors with I-joists and linings made of gypsum plasterboard or wood-based panels, charring phase 3 is the most likely charring phase near failure of the floor.

It is assumed that the cavity is completely filled with batt-type rock fibre or glass fibre and that the insulation does not fall off after failure of the cladding. Since rock fibre insulation is more heat resistant than glass fibre, the model is strictly valid for rock fibre insulated floors only, while it is restricted to the stage before failure of the cladding when glass fibre insulation is used. This limitation, however, implies a considerable under-prediction of the fire resistance of glass fibre insulated floors, since no data were available to achieve better agreement between the design model and test results.

Normally, for reasons of noise protection, the lining is attached to resilient channels made of cold-formed steel or wooden battens with resilient fixing to the joists, creating a void space of 25 mm or more between the cladding and the I-joists and insulation. The model does not explicitly take into account that heat transfer is somewhat lagging behind. On the other hand, from full-scale testing of floors it is known that this void space has a negative effect on the fire resistance of floors, since the spread of fire in horizontal direction will increase once there is a local penetration of the fire through joint-openings in the cladding or when the first small pieces of the cladding start to fall off [4]. The beneficial effect of resilient channels is that they support the insulation between the I-joists, provided that the fixing of the resilient channel is effective. This will require sufficient length of screws or nails to ensure penetration into unburnt wood.

The charring and mechanical properties of I-joists are determined in two steps. The charring properties are determined using the residual cross-section from the thermal analysis, assuming that all parts of the cross-section with temperatures greater than 300°C have undergone charring. The notional charring depth, $d_{\mathrm{char,n}}$, of the fire exposed flange is determined, assuming that

- the notional residual cross-section of the fire exposed flange is rectangular and the flange width is equal to the original flange width b;
- the section modulus of notional residual cross-section, W_{r}, is equal to the residual cross-section obtained by the thermal analysis.

2.2 Resistance of I-joists

2.2.1 Cross-section

The dimensions of an I-joist are shown in Figure 2.3. At ambient temperature, the characteristic moment resistance is calculated as:

$$M_{\mathrm{k}} = f_{\mathrm{m,k}}\, W_{\mathrm{ef}}\, k_{\mathrm{h}} \tag{2.1}$$

with

$$W_{\mathrm{ef}} = \frac{2I_{\mathrm{ef}}}{h} \tag{2.2}$$

$$I_{\mathrm{ef}} = I_{\mathrm{f}} + \frac{E_{\mathrm{w}}}{E_{\mathrm{f}}} I_{\mathrm{w}} \tag{2.3}$$

where:

$f_{\mathrm{m,k}}$ is the characteristic bending strength of the I-joist, se below;

E_{f} is the mean value of the modulus of elasticity of the flange;

E_{w} is the mean value of the modulus of elasticity of the web;

I_{f} is the contribution of the flanges to the second moment of area;

I_{w} is the contribution of the web to the second moment of area

k_{h} is a depth effect where applicable, see below.

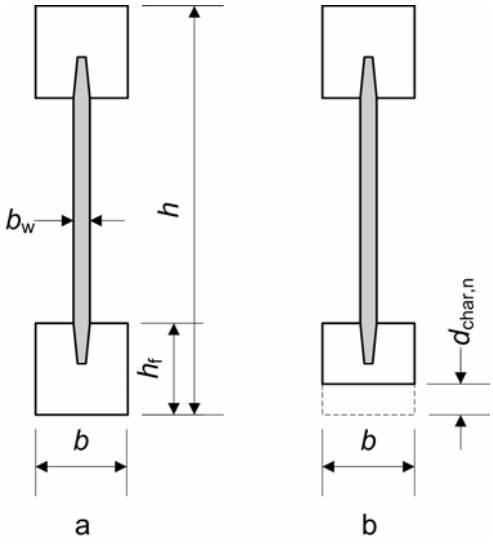

Figure 2.3: Cross-section of I-joist, a: at ambient conditions, b: in the fire situation

When the bending resistance of the I-joist is calculated according to EN 1995-1-1 [5], $k_{\mathrm{h}} = 1$ and the characteristic bending strength of the I-joist, $f_{\mathrm{m,k}}$, is taken as the bending strength of the flanges. Since the mean flange design stresses $\sigma_{\mathrm{f,c,d}}$ and $\sigma_{\mathrm{f,t,d}}$ should not be greater than the design compressive and tensile strength of the flanges, $f_{\mathrm{m,k}}$ can be replaced by

$$f_{\mathrm{m,k,ef}} = \min \begin{cases} f_{\mathrm{m,k}} \\ \dfrac{f_{\mathrm{c,k}}\, h}{h - h_{\mathrm{f}}} \\ \dfrac{f_{\mathrm{t,k}}\, h}{h - h_{\mathrm{f}}} \end{cases} \tag{2.4}$$

Where the bending resistance of the I-joist was derived from testing, the characteristic bending strength of the I-joist, $f_{\mathrm{m,k}}$, and k_{h} are declared by the producer of the I-joist.

In the fire situation, for I-beams in floor assemblies with cavities that are completely insulated, the cross-section shown in Figure 2.3b should be used to calculate the mechanical resistance for the required period of fire exposure t.

For failure during charring phase 3, that is the cladding has fallen off at the time t_f, the notional charring depth, $d_{char,n}$, should be taken as:

$$d_{char,n} = \beta_n \, (t - t_{f,ef}) \tag{2.5}$$

where:

$$\beta_n = \beta_0 \, k_{b,ch} \, k_3 \, k_n \tag{2.6}$$

$$k_{b,ch} = \frac{27,4}{b} + 1 \tag{2.7}$$

$$k_3 = 0,0157 \, t_f + 1 \tag{2.8}$$

$$t_{f,ef} = 0,9 \, t_f \tag{2.9}$$

$$k_n = 1,4$$

β_0 is the one-dimensional charring rate given in EN 1995-1-2 [1], that is β_0 = 0,65 mm/min for solid softwood and LVL;

t_f is the failure time of the cladding, in mm; it may be given by EN 1995-1-2 or by the producer or be determined with respect to withdrawal failure cladding fasteners, see 2.2.2;

$t_{f,ef}$ is the effective failure time of the cladding;

b is the flange width in mm.

For failure during charring phase 2, that is failure takes place at or before the time of failure of the cladding, the notional charring depth, $d_{char,n}$, should be taken as:

$$d_{char,n} = \beta_n \, (t - t_{ch}) \tag{2.10}$$

where:

$$\beta_n = \beta_0 \, k_{b,ch} \, k_2 \, k_n \tag{2.11}$$

and $k_2 = 1$.

2.2.2 Failure of cladding fasteners

The penetration length into unburnt wood of fasteners for fixing claddings or resilient channels should be at least 10 mm. The charring depth may be taken as the notional charring depth $d_{char,n}$, see Figure 2.4.

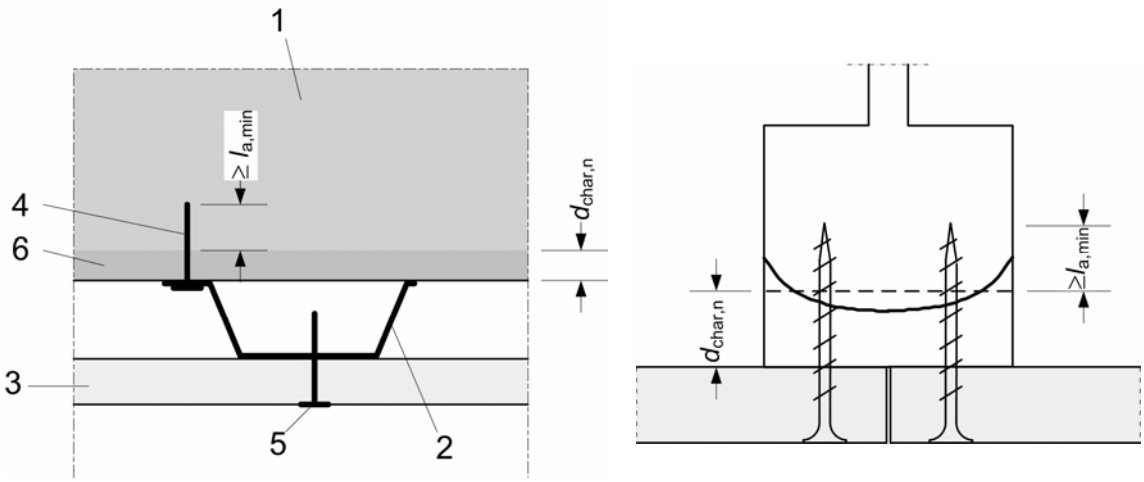

Key:
1 Timber member
2 Steel channel
3 Panel
4 Fastener for fixing of steel channel to timber member
5 Fastener for fixing of panel to steel channel
6 Char layer

Figure 2.4: a) Fixing of resilient channels to timber member (from EN 1995-1-2 [1]), b) Fixing of gypsum plasterboard to timber member

2.2.3 Strength parameters

2.2.3.1 General

EN 1995-1-2 gives the design value of strength parameters as:

$$f_{\mathrm{d}} = k_{\mathrm{mod,fi}} \frac{f_{20}}{\gamma_{\mathrm{M,fi}}} \tag{2.12}$$

where:

f_{20} is the 20 % fractile of the strength property at ambient temperature;

$k_{\mathrm{mod,fi}}$ is a modification factor, taking into account the reduction of the strength at elevated temperatures;

$\gamma_{\mathrm{M,fi}}$ is the material partial safety factor for the fire situation.

The 20 % fractile of the strength property at ambient temperature is taken as:

$$f_{20} = k_{\mathrm{fi}}\ f_{\mathrm{k}} \tag{2.13}$$

where f_{k} is the characteristic strength property and

$$k_{\mathrm{fi}} = \begin{cases} 1,25 & \text{for solid timber} \\ 1,1 & \text{for LVL} \end{cases}$$

2.2.3.2 Bending resistance

For I-joists in bending where the fire-exposed flange is in tension, the modification factor for bending strength, $k_{\text{mod,fm,fi}}$, should be calculated as:

$$k_{\text{mod,fm,fi}} = 1 - 0,016\, d_{\text{char,n}}\, k_{\text{b,fm}}\, k_{\text{hf,fm}}\, k_{\text{h,fm}} \tag{2.14}$$

with

$$k_{\text{b,fm}} = 0,76 + \frac{11,5}{b} \tag{2.15}$$

$$k_{\text{hf,fm}} = \frac{68}{h_{\text{f}}} - 0,41 \tag{2.16}$$

$$k_{\text{h,fm}} = 1,4 - \frac{80}{h} \tag{2.17}$$

where the notional charring depth $d_{\text{char,n}}$, the flange width b, the flange depth h_{f} and cross-section depth h are in mm.

2.2.3.3 Shear resistance

For shear strength verification of the web, the maximum temperature of the web should be calculated as:

$$\Theta_{\text{w,max}} = \frac{160\, k_{\text{b}}\, d_{\text{char,n}}}{h_{\text{f}}} - 47 \tag{2.18}$$

For wood-based webs the modification factor for shear strength, $k_{\text{mod,fv,fi}}$, may be calculated, using the reduction factor for shear strength given in Figure B4 of EN 1995-1-2 [1], as:

$$k_{\text{mod,fv,fi}} = \begin{cases} 1 & \text{for} \quad \dfrac{48\, k_{\text{b,ch}}\, d_{\text{char,n}}}{h_{\text{f}}} \le 20 \\ 1,47 - \dfrac{1,13\, k_{\text{b,ch}}\, d_{\text{char,n}}}{h_{\text{f}}} & \text{for} \quad \dfrac{48\, k_{\text{b,ch}}\, d_{\text{char,n}}}{h_{\text{f}}} > 20 \end{cases} \tag{2.19}$$

For shear strength verification of the glue-line between the web and the flange, the temperature in degrees Celsius should be taken as:

$$\Theta_{\text{joint}} = \max \begin{cases} 666\, d_{\text{char,n}}\, \dfrac{k_{\text{b}}}{\sqrt{b}\, h_{\text{f}}} - 12 \\ 20 \end{cases} \tag{2.20}$$

where $d_{\text{char,n}}$, b and h_{f} are in mm.

3 Determination of model parameters

3.1 Methodology

The charring and mechanical properties of I-joists were determined in two steps. The charring properties were determined using the residual cross-section from the thermal analysis, assuming that all parts of the cross-section with temperatures greater than 300°C have undergone charring. Since the irregular shape of the residual cross-section of the fire-exposed flange is unfavourable for use in design calculations, a notional charring depth, $d_{\text{char,n}}$, of the fire exposed flange was determined (see Figure 3.1), assuming that:

- the notional residual cross-section of the fire exposed flange is rectangular and the flange width is equal to the original flange width b;
- the section modulus of notional residual cross-section, W_{r}, is equal to the residual cross-section obtained by the thermal analysis.

Since the bending moment resistance of a fire-exposed beam is dependent on charring and bending strength reduction (see Figure 3.11), the modification factor for the reduction of bending strength, $k_{\text{mod,fm,fi}}$, was determined from

$$k_{\text{mod,fm,fi}} = \frac{M_{\text{fi}}\, W}{M\, W_{\text{r}}} \tag{3.1}$$

where:

M is the bending moment resistance under ambient conditions;

M_{fi} is the bending moment resistance in the fire situation;

W_{r} is the section modulus of the residual cross-section of the I-joist;

W is the section modulus of the original cross-section of the I-joist.

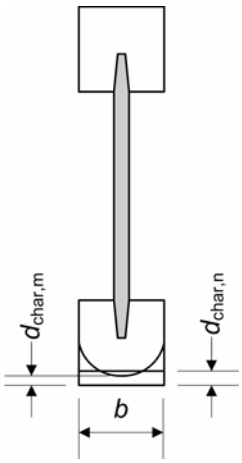

Figure 3.1 – Determination of the notional (equivalent) charring depth

A typical cross-section of an I-joist is shown in Figure 3.2a. Most calculations were conducted for an I-joist (H200) with h = 200 mm, b = 48 mm, h_{fl} = 48 mm and b_{w} = 8 mm. Thereafter the flange width was varied from 36 to 88 mm and the depth of the cross-section was increased to 300 mm. With respect to the web properties some simplifying assumptions were made. The flanges of I-joists and studs are produced using solid timber or engineered wood products such as LVL, while the web is normally made of wood-based panels (particleboard, OSB or wood fibreboard). Since the effect of the web is small on both temperature development in the web and the resistance of the cross-section, see Figure 3.3, (the modulus of elasticity of the web is between 20 and 50 % of the modulus of elasticity of the flanges), the modulus of elasticity of the web was taken equal to zero in the bending resistance analysis and the determination of the notional charring depth, see Figure 3.2b, while thermal properties of wood were assumed for the web in the thermal analysis, see Figure 3.2c. Further, the bonded-in part of the web was given the same properties as the flange; this simplification compensates, to some extent, for the effects of disregarding the web.

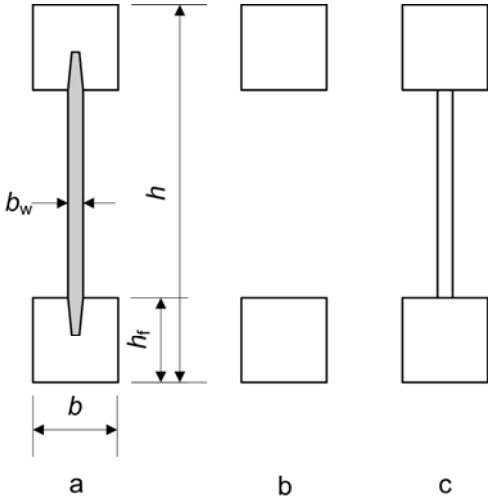

Figure 3.2 – a) Dimensions of I-shaped section, b) Cross-section for mechanical analysis (bending) and determination of notional charring depth, c) Cross-section for thermal analysis

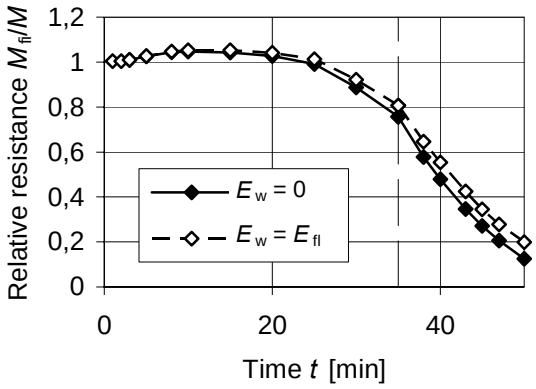

Figure 3.3 – Example of effect of web properties on relative bending resistance (failure of cladding after 35 minutes, see case 3b of Table 1)

Although floor and wall assemblies always include claddings on the fire exposed side, calculations were also conducted on assemblies consisting of an I-joist plus the cavity insulation (without cladding). The results of these calculations were used for studying the effect of parameters such as the flange width, flange depth and the total depth of the cross-section.

3.2 Thermal analysis

3.2.1 Software and discretisation

The thermal analysis was executed using the software SAFIR 2004 [6]. This version of SAFIR permits modelling the failure of claddings at specific times, e.g. when a pre-defined failure criterion has been reached (a specific temperature on the unexposed side of gypsum plasterboard linings, or pull-out failure of fasteners, or a value known from full-scale fire tests), by using the temperature field from the first run as start temperature field in the following calculation without the cladding that is assumed to have fallen off.

For the thermal analysis a grid was used with element sizes from 2 mm × 2 mm to 8 mm × 8 mm, see Figure 3.4.

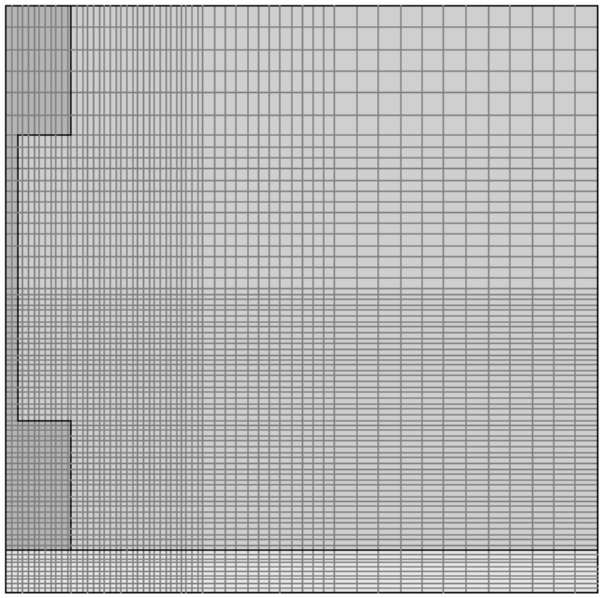

Figure 3.4 – Discretisation for the thermal analysis: I-joist with h = 200 mm, b_{fl} = 48 mm, h_{fl} = 48 mm, b_w = 8 mm and cladding h_p = 15,4 mm. The cladding on the ambient side was neglected

3.2.2 Thermal properties

In the heat transfer calculations, the thermal properties of timber were taken from EN 1995-1-2 [1], based on [7]. The heat capacity values of gypsum plasterboard were taken from Sultan [8], whereas the thermal conductivity values were modified to fit the test results by König and Rydholm [9] on 95 mm thick timber slabs protected by Swedish gypsum plasterboard of types A or F in accordance with EN 520 [10], see Figure 3.5. For the insulation material the thermal properties were taken from Källsner and König [11].

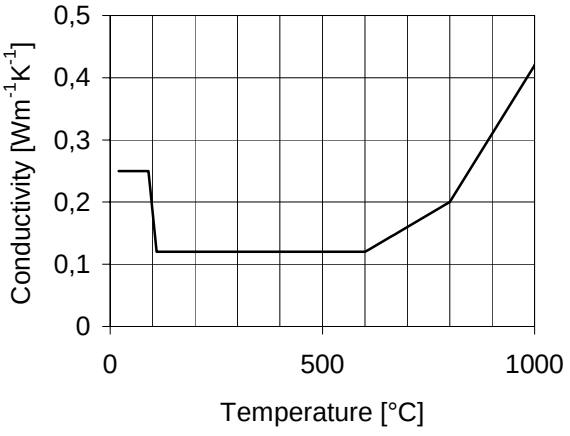

Figure 3.5 – Thermal conductivity of gypsum plasterboard

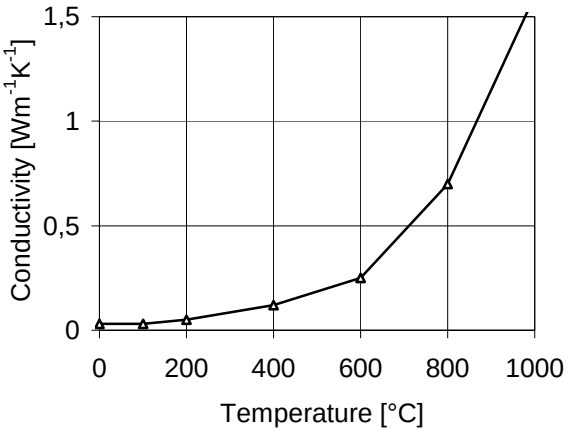

Figure 3.6 – Thermal conductivity of insulation

An example of typical results of the thermal analysis is shown in Figure 3.7. The graph indicates a rounded shape of the residual cross-section of the fire exposed flange; the char-line of which is defined as the location of the 300°C isotherm. Of special interest is the charring depth in the middle of the flange (axis of symmetry of the cross-section), $d_{char,m}$. The char development for the I-shaped section H200 is shown below, see Figure 3.12.

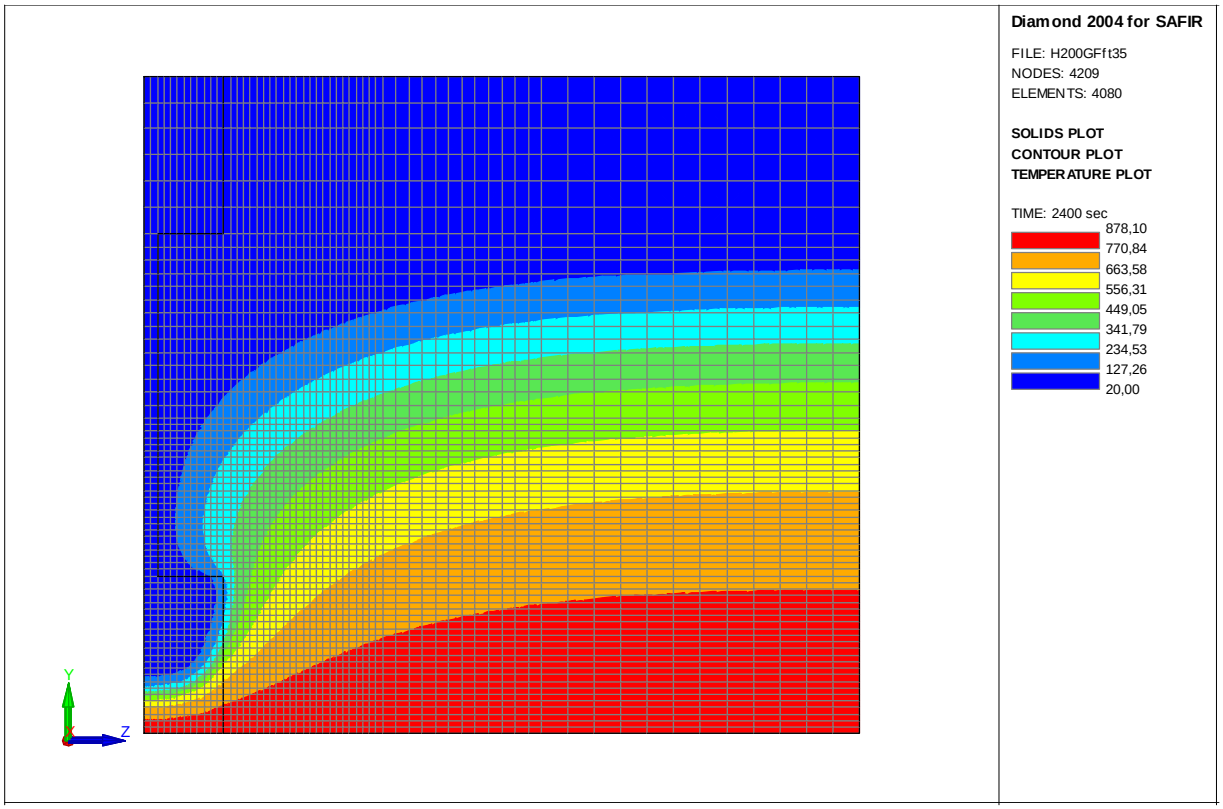

Figure 3.7 – Example of temperature field of assembly at 40 minutes, 5 minutes after failure of fire protective cladding

3.3 Structural analysis

3.3.1 Software

For the structural analysis, a computer program CSTFire, written as a Visual Basic macro embedded in Excel, was developed, using the temperature output from the heat transfer calculations and the relative strength and stiffness values given by EN 1995-1-2 [1], i.e. compressive and tensile strengths, f_c and f_t, and moduli of elasticity in compression and tension, E_c and E_t. These values are given as bi-linear functions of temperature from 20 to 300°C with breakpoints at 100°C, also taking into account the effects of transient moisture situations and creep, see Figure 3.8. The software takes into account the possibility of permitting ductile behaviour of wood under elevated temperature. Contrary to ambient conditions where failure on the tension side of a beam is brittle, in the fire situation tensile failure of the outermost fibres won't cause immediate collapse of the member since a redistribution of internal stresses will take place as long as equilibrium is maintained.

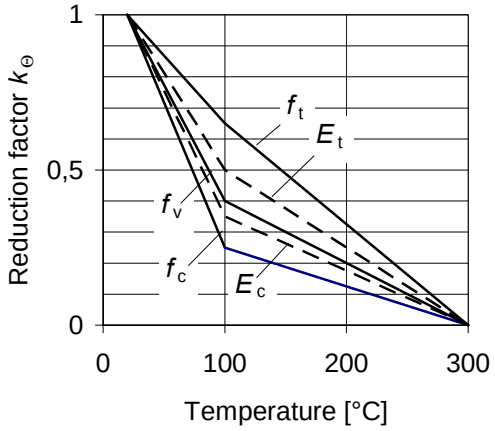

Figure 3.8 – Reduction factors for strength and stiffness properties according to EN 1995-1-2

Since the reduction of strength and stiffness properties is different for tension and compression, CSTFire uses an iteration process, increasing the curvature of the member until the maximum moment resistance is reached. The element size used for the structural analysis was chosen as 1 mm × 1 mm. Since a coarser grid was used in the thermal analysis, intermediate temperature values were determined by linear interpolation.

3.3.2 Material properties

The calculations were conducted assuming material properties that are representative for I-shaped sections used in practice, using the stress-strain relationship shown in Figure 3.9. Since the values of tensile and compressive strength of solid timber given in design or product standards, e.g. EN 338 [12], are values of the whole cross-section and were determined on the assumption of a linear relationship between stress and strain until failure, the use of these values in a finite element analysis would not be correct. Therefore, compressive strength values were determined using the data from Thunell [13] giving the compressive strength of clear pine wood (pinus sylvestris) for different moisture contents and dry densities up to 350 kg/m^3. These values can be expressed as:

$$f_c = 0{,}114\,\rho_{0,12} - 9 \qquad (3.2)$$

where $\rho_{0,12}$ is the dry density of wood in kg/m^3, based on the volume of the wood at a moisture content of 12 %. For the I-joists assumed here with solid timber flanges of a quality slightly better than strength class C30 according to EN 338 [12], the producer declared a bending strength f_m of 27 N/mm^2. For strength class C30 the characteristic density including 12 % moisture is 380 kg/m^3, that is the dry density is 339 kg/m^3 and, with expression (2), the compressive strength is 29,7 N/mm^2. In the calculations the rounded value of f_c = 30 N/mm^2 was used. Since $f_c > f_m$, the bending stresses over the depth are linearly distributed. Therefore we can assume $f_t = f_m$ = 27 N/mm^2. For I-joists with the tension flange on the fire exposed side, from the calculations below could be seen that there is no influence of compressive strength on the results as long as it is greater than the tensile strength.

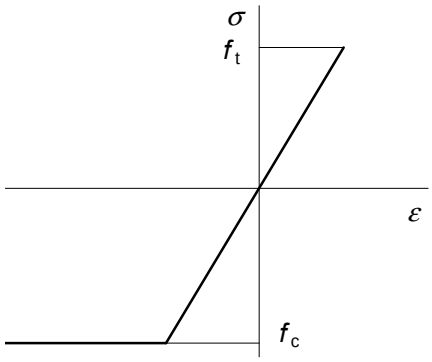

Figure 3.9 – Stress-strain relationships of wood

3.4 Effect of protection and charring phase

3.4.1 Bending resistance

Calculations were made of an I-shaped section H200 with the dimensions h = 200 mm, b = 48 mm and h_f = 48 mm. The tension flange was on the fire exposed side of the I-joist, either unprotected or protected by various gypsum plasterboard claddings. In the calculations, different failure times of the claddings were assumed, see Table 1. GA and GF refer to type A and F respectively in accordance with EN 520 [10]. In all cases the cavities were completely filled with rock fibre insulation that was assumed to remain in place after failure of the claddings. In Figure 3.10 the results of the calculations are shown as relative resistances versus time for different cases, see Table 1. Case 1 serves as a reference scenario to demonstrate the effect of the claddings, although this will never be used in practice. In all cases 1, 2, 3 and 4, the resistance initially increases above the values at ambient temperature since the wood on the fire exposed tension side becomes ductile at elevated temperatures, permitting the redistribution of internal stresses utilizing the fact that compressive strength is larger than the tensile strength and/or the material is assumed as elastic-plastic in compression, see Figure 3.9. This has, however, no influence on the final bending resistance under fire exposure.

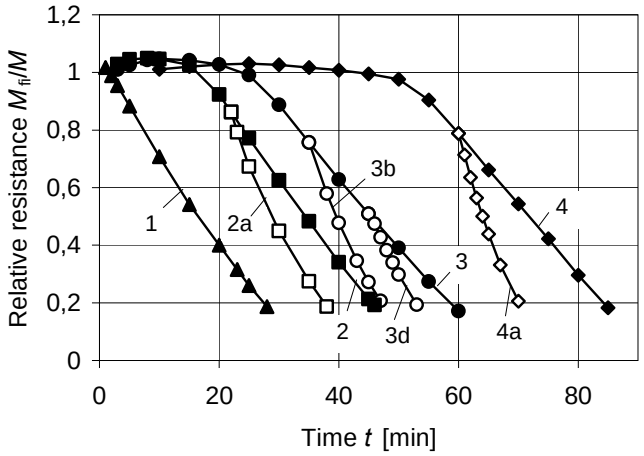

Figure 3.10 – Relative resistance of I-joist H200 with different gypsum plasterboard claddings and different failure scenarios assumed for claddings, see Table 1

Table 1 – Assemblies and failure scenarios of claddings

Case	**Cladding**	**Failure time of cladding** t_f min
1	none	
2	12,5 mm GA	none
2a	12,5 mm GA	21
3	15,4 mm GF	none
3a	15,4 mm GF	32
3b	15,4 mm GF	35
3c	15,4 mm GF	40
3d	15,4 mm GF	45
4	12,5 mm GA + 15,4 mm GF	none
4a	12,5 mm GA + 15,4 mm GF	60
4b	12,5 mm GA + 15,4 mm GF	70

For load ratios relevant in practice, that is between 0,2 and 0,4, the contribution of charring and strength degradation to the reduction of bending resistance are of about the same order of magnitude, see Figure 3.11.

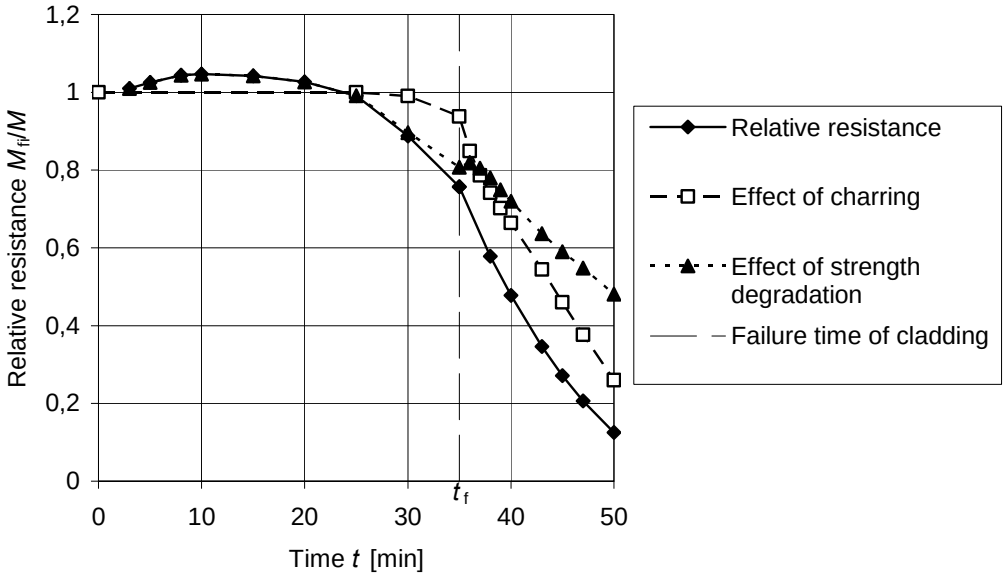

Figure 3.11 – Example of influence of charring and strength degradation on bending resistance (case 3b)

3.4.2 Charring depth and charring rates

From the temperature field within the I-joist obtained from the heat transfer analysis, the charring depth was determined, using the 300°C isotherm as the char-line. The propagation of the char front is illustrated in Figure 3.12.

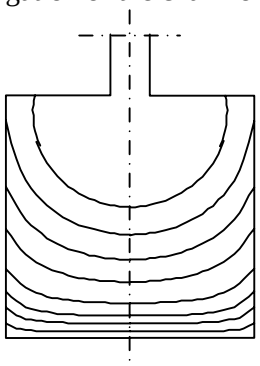

Figure 3.12 – Propagation of char front in fire-exposed flange

Relationships of charring depth in the middle of the flange versus time are shown in Figure 3.13. For curve numbers, see the different cases given in Table 1. Again case 1 (initially unprotected by a cladding) serves as the reference scenario. In cases without failure of the cladding, after some time charring starts at time t_{ch}, initially at a lower rate than in case 1 (charring phase 1), but later on with an increasing rate. When the cladding fails at time t_f, an immediate increase of the charring rate takes place, however after a few minutes the charring rate has slowed down and stabilized (charring phase 3), but it is greater than the charring rate during charring phase 1. For simplicity, the non-linear relationships were replaced by secant values for $d_{char,m}$ = 20 mm, see Figure 3.14. When the charring has reached that value, the resistance is about 0,3 of the value at ambient temperature. Thus secant value of the charring rate gives slightly conservative results at load levels that are common in practice and slightly non-conservative values for lower resistances.

For charring phase 2, that is for cases 2, 3 and 4, the ratio k_2 was determined as

$$k_2 = \frac{\beta_{char,m,2}}{\beta_{char,m,1}} \tag{3.3}$$

where $\beta_{char,m,1}$ and $\beta_{char,m,2}$ are the charring rates in the middle of the flange for charring phases 1 and 2 respectively, that is the slopes of the secant relationships shown in Figure

3.14. Since the values are close to unity, see Figure 3.15, it is proposed to use $k_2 = 1$ in all cases of charring phase 2.

For charring phase 3 after failure of the cladding, the best fit was obtained by introducing an effective failure time of the panel, $t_{f,ef}$, (see Figure 3.14), determined as 90 % of the actual failure time (see Figure 3.16).

For charring phase 3, that is for cases 2a, 3a, 3b, 3c, 3d, 4a and 4b, the ratio k_3 was determined as

$$k_3 = \frac{\beta_{char,m,3}}{\beta_{char,m,1}} \tag{3.4}$$

where $\beta_{char,m,1}$ and $\beta_{char,m,3}$ are the charring rates in the middle of the flange for charring phases 1 and 3 respectively. The results can be expressed as a trendline given by (see Figure 3.17):

$$k_3 = 0,0157\, t_f + 1 \tag{3.5}$$

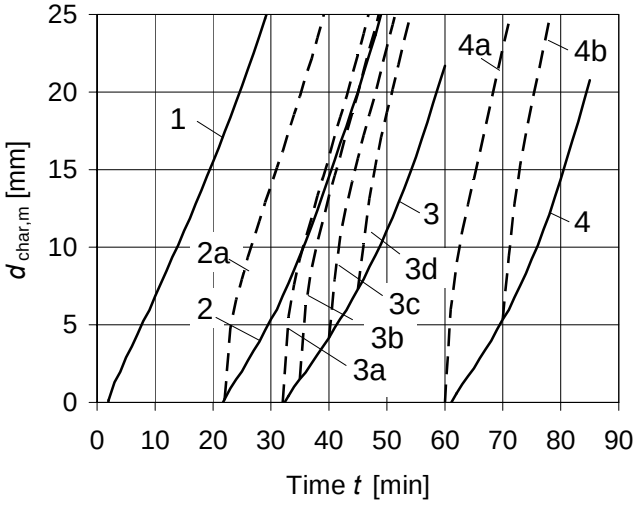

Figure 3.13 – Charring depth vs. time in the middle of the flange

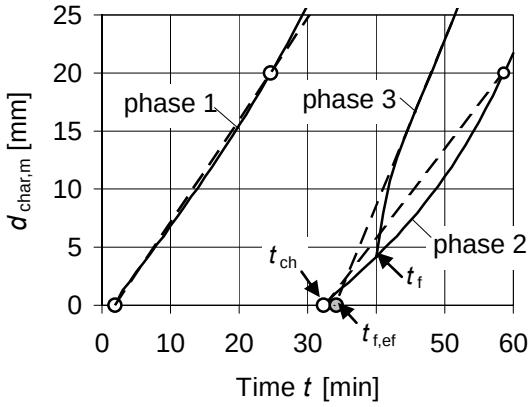

Figure 3.14 – Modelling of charring depth by linearization at different charring phases 1, 2 and 3

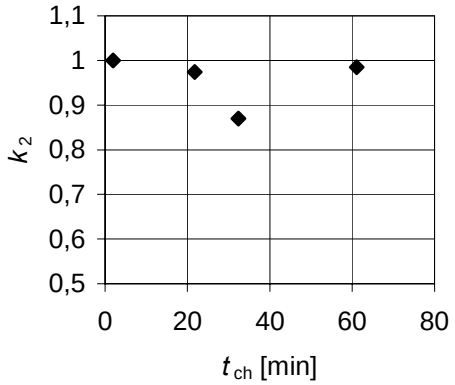

Figure 3.15 – Ratio k_2 vs. time of start of charring

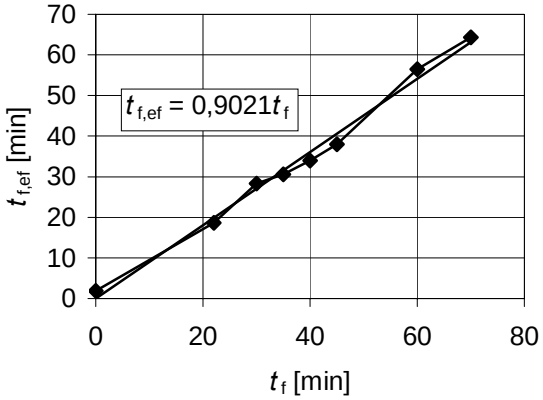

Figure 3.16 – Determination of effective failure time of cladding

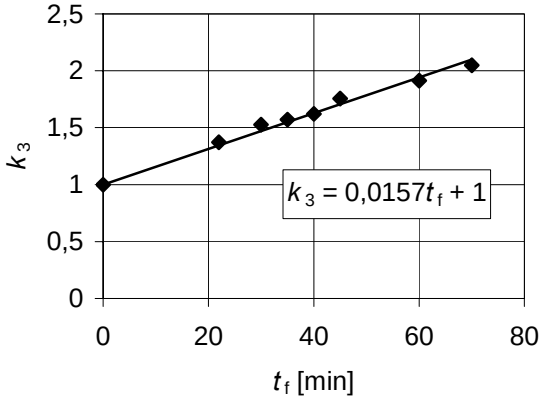

Figure 3.17 – Determination of k_3 for charring phase 3 after failure of cladding

Replacing the real residual shape of the cross-section with a rectangular cross-section with width b, a notional charring depth, $d_{char,n}$ was determined, see Figure 2.3. Relationships of the notional charring depth vs. time are shown in Figure 3.18.

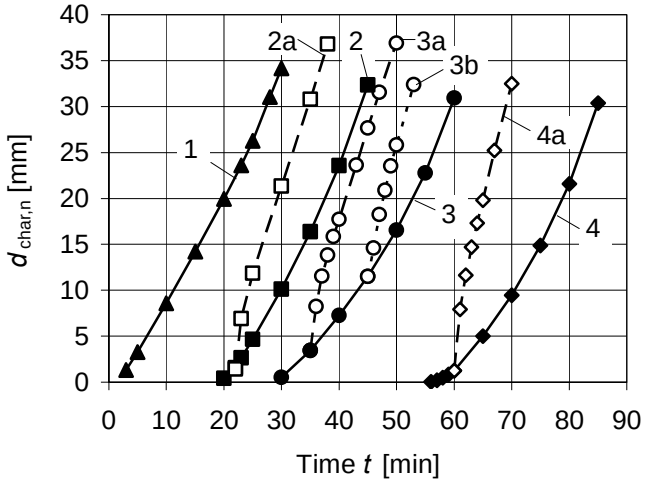

Figure 3.18 – Notional charring depth vs. time

The ratio

$$k_{\mathrm{n}} = \frac{d_{\mathrm{char,n}}}{d_{\mathrm{char,m}}} \tag{3.6}$$

between the notional charring depth as a function of the charring depth in the middle of the flange is shown in Figure 3.19. For curves representing charring phase 3 which is the most likely scenario in floors, a general value of k_{n} = 1,4 can be used.

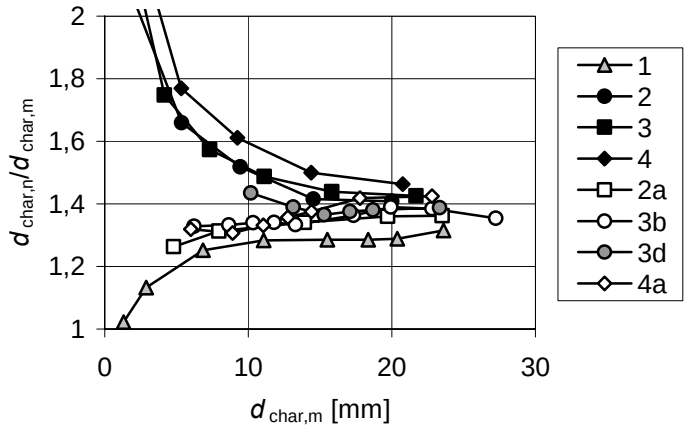

Figure 3.19 – Relationship of k_{n} vs. $d_{\mathrm{char,m}}$

From Figure 3.19 we can see that there is some influence of the charring phase on k_{n}, depending on different shapes of the residual cross-sections during different charring phases, see Figure 3.20. In the figure, three char-lines are compared at a stage when the charring depth in the middle of the flange is 12 mm. For greater charring depths, and close to failure of the I-joist, this difference is considerably smaller, see Figure 3.19.

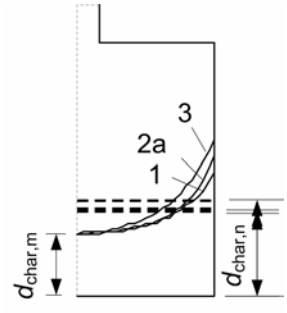

Figure 3.20 – Real and notional charring depths in the flange for charring phases 1 (curve 1), 2 (curve 3) and 3 (curve 2a); for numbering of the curves, see Table 1

3.4.3 Modification factor for bending strength

The modification factor for bending strength, $k_{mod,fm,fi}$, determined according to equation (3.1), is shown in Figure 3.21 as a function of the notional charring rate. There exists a considerable effect of the scenarios chosen; for I-joists during charring phase 2, that is the gypsum plasterboard cladding remains attached to the joists, bending strength reduces more than for joists during charring phase 1 (initially unprotected) or charring phase 3 after failure of the cladding. Immediately after failure of the cladding, $k_{mod,fm,fi}$ is almost constant while the charring depth increases rapidly, see Figure 3.13. After some minutes the charring rate decreases somewhat and $k_{mod,fm,fi}$ decreases at approximately the same rate as during charring phase 2. An explanation of this effect is that the temperature gradient largely depends on the charring rate: at smaller charring rates as during charring phase 2 greater parts of the flange are affected by elevated temperature, and vice versa, at very large charring rates as in charring phase 3, the temperature affected zone is small, see Figure 3.22, showing temperature profiles below the char-line for $d_{char,m}$ = 12 mm. Since charring phase 3 is the most likely scenario for failure of floors in fire, a relationship of $k_{mod,fm,fi}$ was fitted to the most unfavourable of the curves for charring phase 3, see Figure 3.23. The proposed model is given by:

$$k_{mod,fm,fi} = 1 - 0,016\, d_{char,n} \tag{3.7}$$

The distributions of stresses, strengths and temperatures along the axis of symmetry are shown in Figure 3.24 to 3.27. From Figure 3.27 we can see that tensile failure has occurred in a zone close to the char-line.

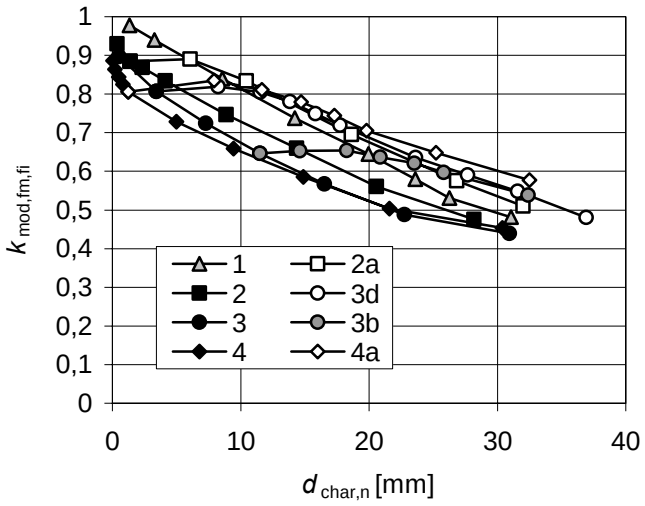

Figure 3.21 – Modification factors for bending strength vs. notional charring depth

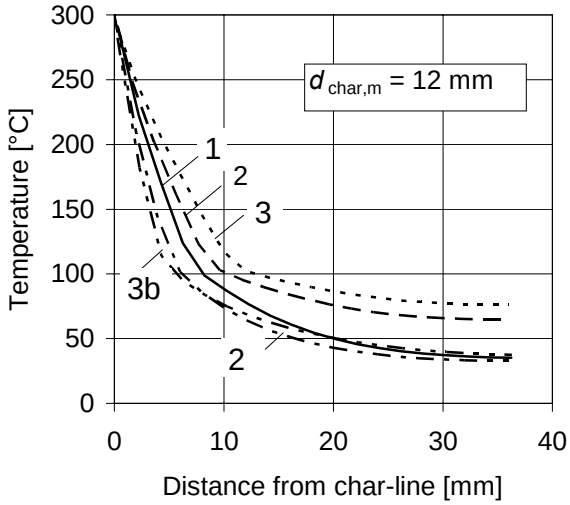

Figure 3.22 – Temperature profiles below char-line along axis of symmetry of flange for $d_{char,m}$ = 12 mm

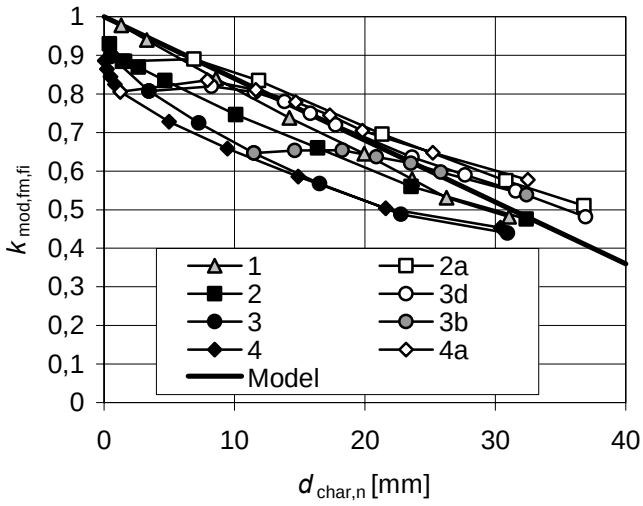

Figure 3.23 – Model of $k_{mod,fm,fi}$

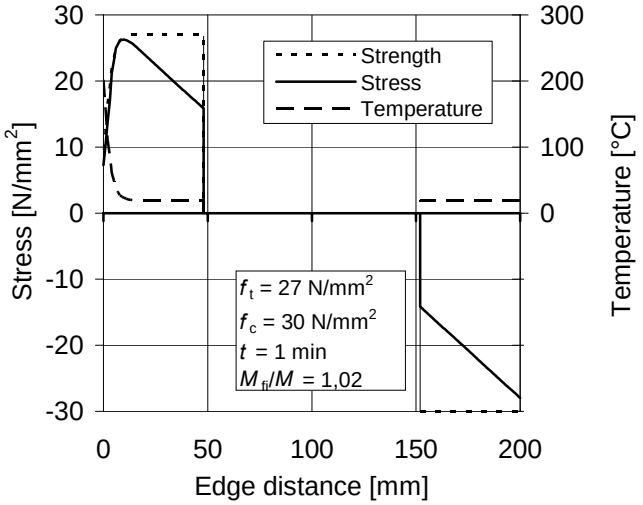

Figure 3.24 –Distribution of stresses, strength and temperature after 1 minute of fire exposure (case 1)

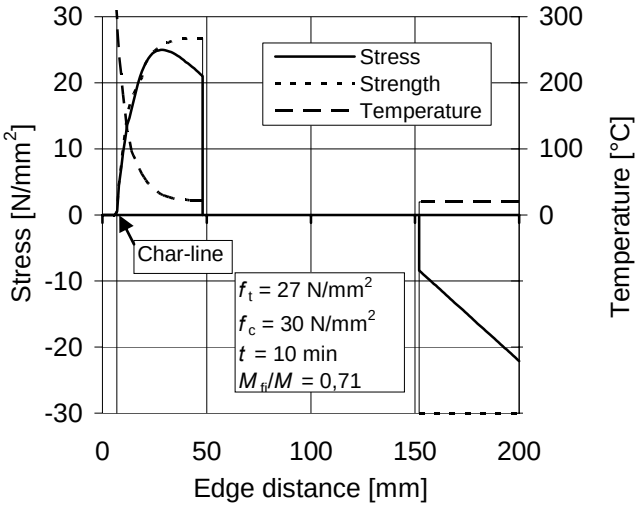

Figure 3.25 – Distribution of stresses, strength and temperature after 10 minutes of fire exposure (case 1)

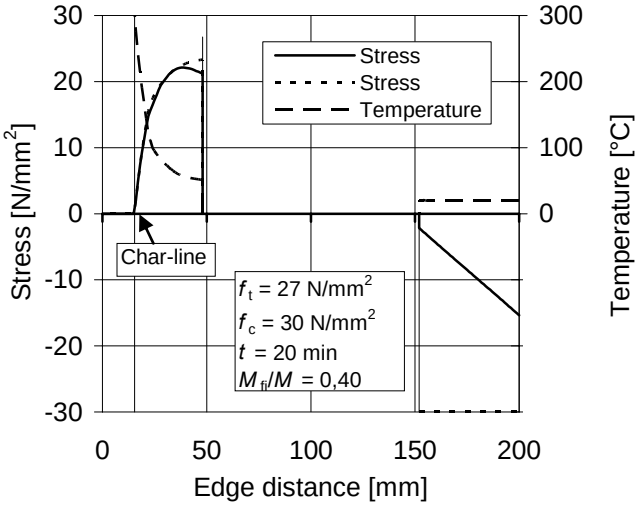

Figure 3.26 – Distribution of stresses, strength and temperature after 20 minutes of fire exposure (case 1)

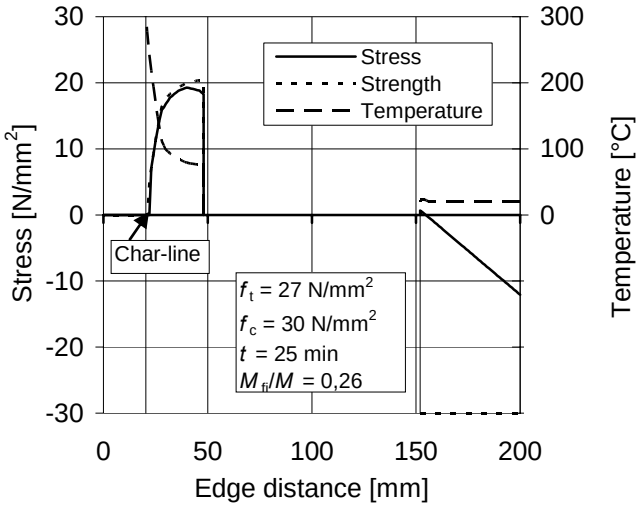

Figure 3.27 – Distribution of stresses, strength and temperature after 25 minutes of fire exposure (case 1)

3.5 Effect of state of stress on the fire exposed side

In single span floors, the fire exposed side of the I-joist is in tension, while in zones near intermediate supports in multiple span floors the fire exposed side is in compression. Whereas the state of stress, tension or compression of the fire exposed parts of the cross-section, does not affect the charring rate [15], there exists a considerable effect on the bending resistance and the modification factor for bending strength, see Figure 3.28 and 3.29. For compression in the fire-exposed flange, the relationships shown in these figures are valid only for braced compression flanges, since the state of stress is fully plastic, see Figure 3.30 where the stress and strength curves are identical on the compression side. Since there is no effective bracing after failure of the cladding, load levels with a high level of yield stresses in the compression flange cannot be utilized. Therefore, instead of showing the stress distribution for the maximum bending resistance as in 3.4.3, in what follows the stress and strength distributions are shown for a load level of 30 % that is more relevant in fire design, see Figure 3.31. After 10 minutes, no yielding has taken place in the flange, while the zone close to the char-line has reached yield strength after 15 minutes. After 20 minutes the compression flange has yielded completely. Since we do not know when an unbraced compression flange would fail in the fire situation, no moment resistance at intermediate supports should be utilized, that is a multi-span floor should be regarded as a series of one-span floors.

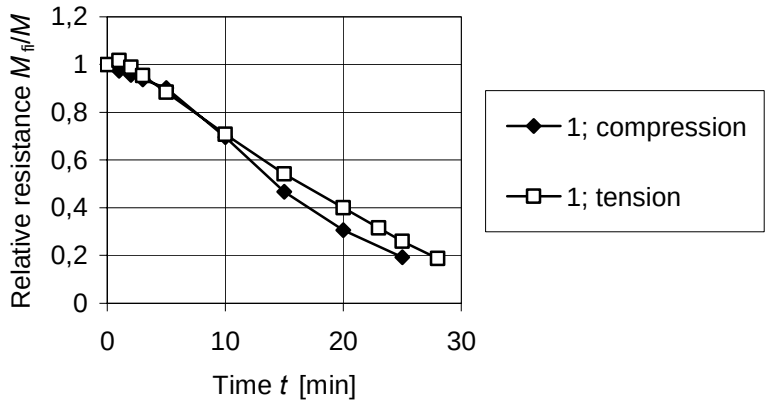

Figure 3.28 – Effect of state of stress in the fire exposed flange on bending resistance

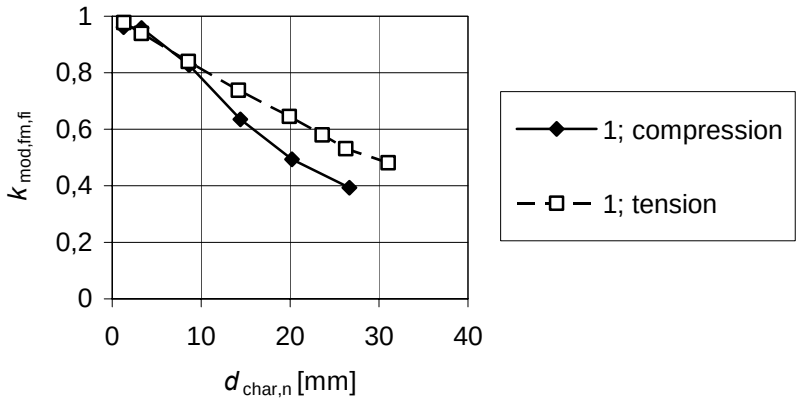

Figure 3.29 – Effect of state of stress in the fire exposed flange on the modification factor for bending strength

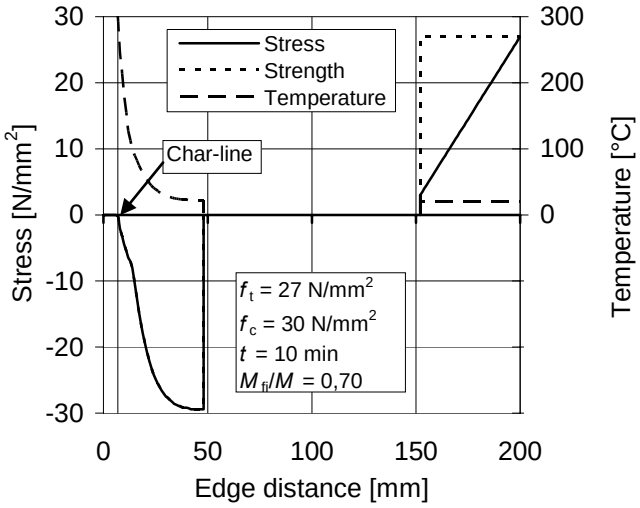

Figure 3.30 – Distribution of stresses, strength and temperature after 25 minutes of fire exposure (case 1) with maximum bending resistance

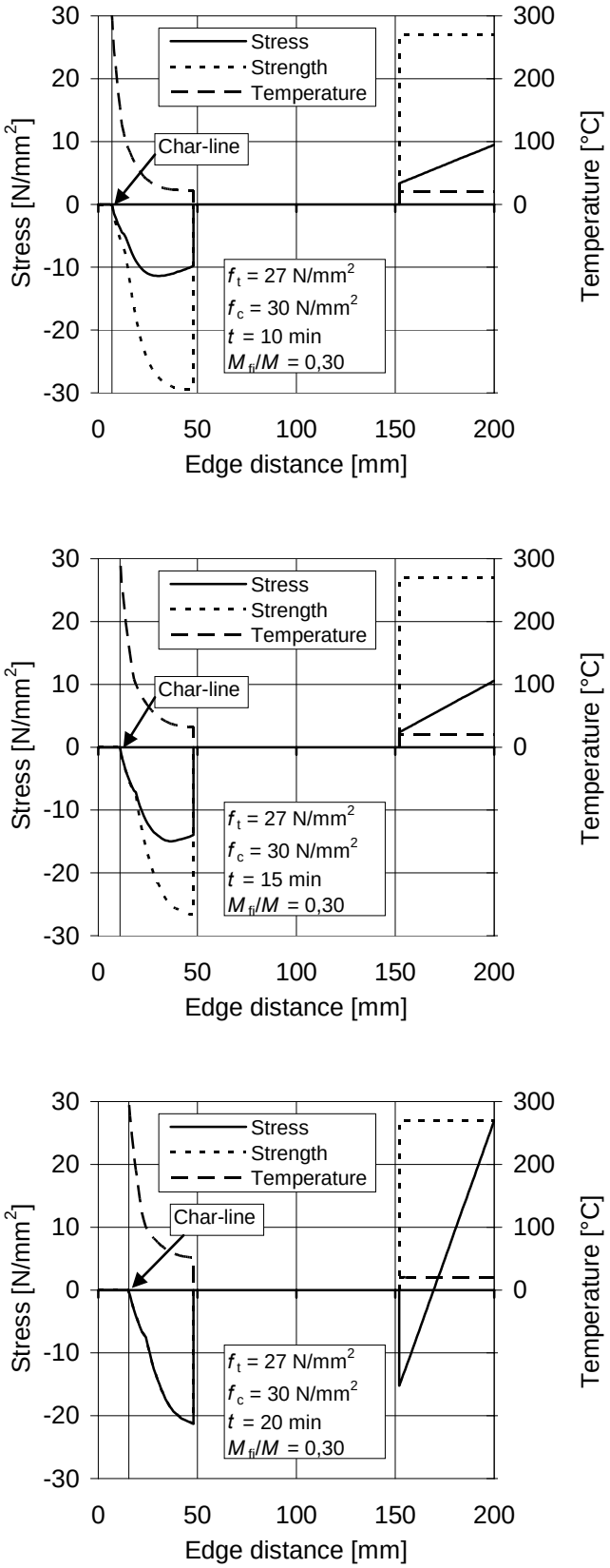

Figure 3.31 – Distribution of stresses, strength and temperature after 10, 15 and 20 minutes of fire exposure (case 1) for a load level of 30 %

3.6 Effect of flange width

3.6.1 Bending resistance and charring

The effect of flange width b was determined, using case 1 with b = 48 mm, h_f = 48 mm and h = 200 mm as the reference cross-section. The cross-section was analyzed using b = 36, 72 and 88 mm. The effect of the flange width on the bending resistance, the charring depth in the middle of the flange and the notional charring depth are shown in Figure 3.32 to 3.35.

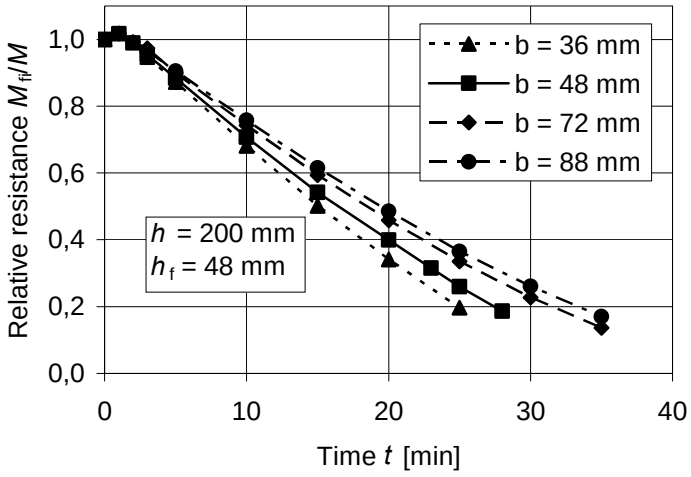

Figure 3.32 – Effect of flange width on bending resistance

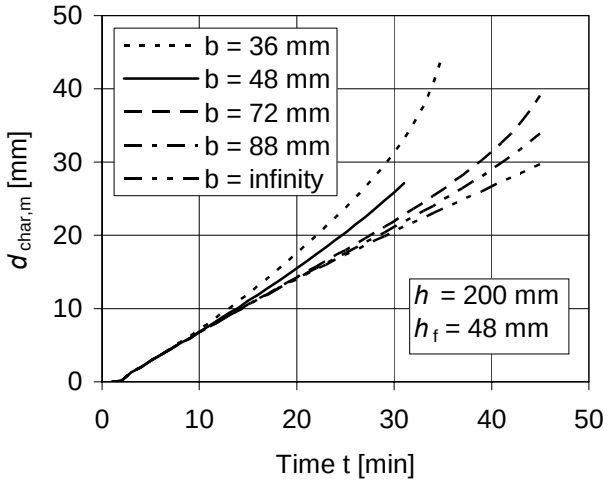

Figure 3.33 – Effect of flange width on the charring depth in the middle of the flange

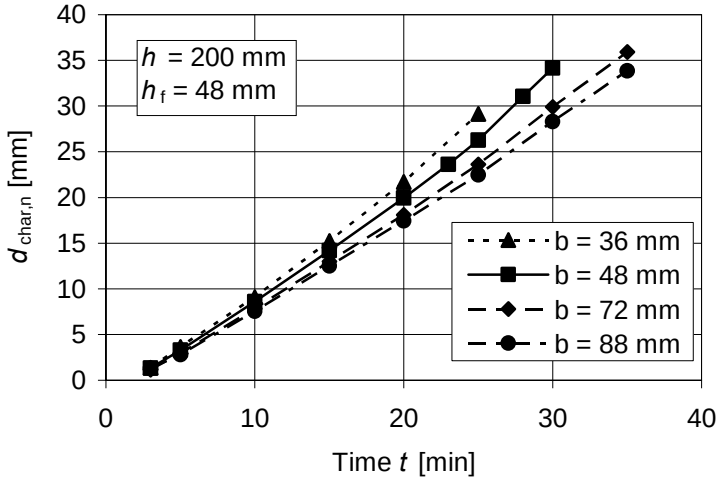

Figure 3.34 – Notional charring depth vs. time

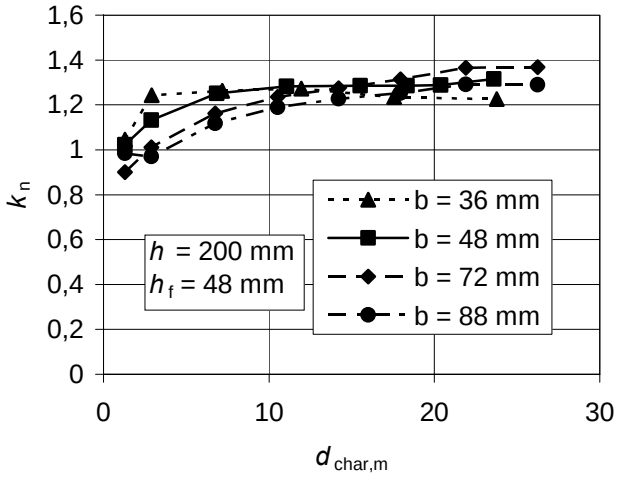

Figure 3.35 – Effect of flange width on the notional charring depth

Using the secant charring values as shown in clause 3.4 the charring rates $\beta_{char,m,b}$ were determined. The ratio $k_{b,ch}$ to be inserted in Equations (2.6) and (2.11) was determined as:

$$k_{b,ch} = \frac{\beta_{char,m,48}}{\beta_{char,m,b}} \tag{3.8}$$

where $\beta_{char,m,48}$ is the charring rate of the reference cross-section with b = 48 mm and $\beta_{char,m,b}$ is the charring rate of the cross-sections with b = 36, 72 and 88 mm respectively. In Figure 3.36 $k_{b,ch}$is plotted against 48/b. The trendline

$$k_{b,ch} = 0,5703 \times \frac{48}{b} + 1 \tag{3.9}$$

can be transformed to

$$k_{b,ch} = \frac{27,4}{b} + 1 \tag{3.10}$$

For b = infinity, $k_{b,ch}$ = 1, that is the charring rate is equal to the one-dimensional charring rate of a semi-infinite slab.

Since the effect of the flange width on the k_n is small (Figure 3.35), it can be neglected.

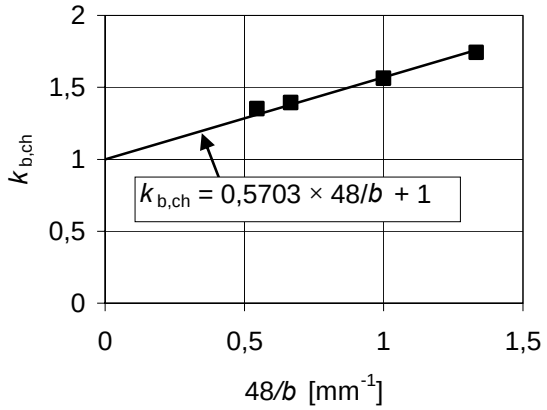

Figure 3.36 – Determination of effect of flange width on charring depth

3.6.2 Modification factor for bending strength

Relationships of the modification factor for bending strength and the notional charring depth are shown in Figure 3.37. Linear relationships expressed by

$$k_{\mathrm{mod,fm,fi}} = 1 - a\, d_{\mathrm{char,n}} \tag{3.11}$$

were fitted to these curves. Using the cross-section with b = 48 mm as a reference, the relative slopes to be inserted in Equation (2.14) were determined as:

$$k_{\mathrm{b,fm}} = \frac{a_b}{a_{48}} \tag{3.12}$$

where a_b is the slope of the curve for width b and a_{48} is the slope for b = 48 mm. The influence of b on the factor $k_{\mathrm{b,fm}}$ is shown in Figure 3.38. A trendline was determined as

$$k_{\mathrm{b,fm}} = 0,24 \times \frac{48}{b} + 0,76 \tag{3.13}$$

and, after modification, as

$$k_{\mathrm{b,fm}} = \frac{11,5}{b} + 0,76 \tag{3.14}$$

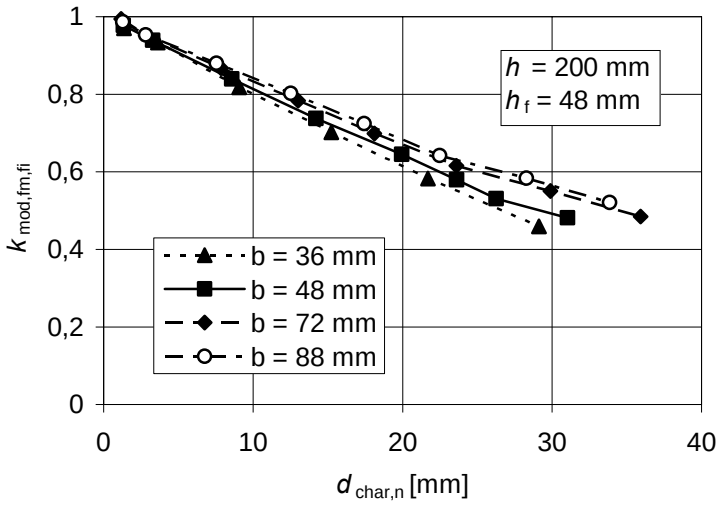

Figure 3.37 – Modification factor for bending strength vs. notional charring depth for various flange widths

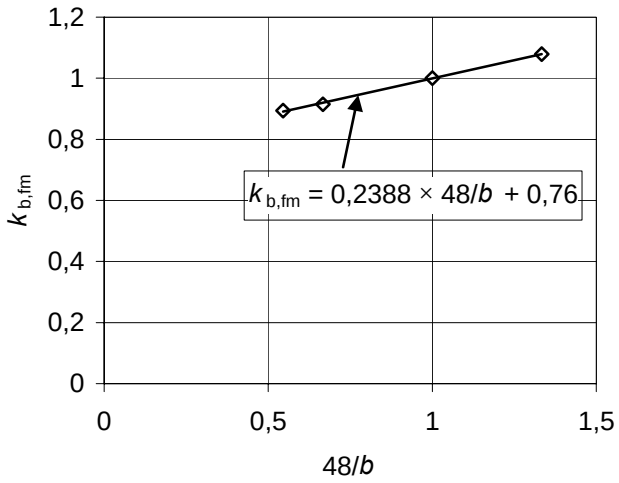

Figure 3.38 – Determination of effect of flange width on bending strength

3.7 Effect of flange depth

3.7.1 Bending resistance and charring

The influence of flange depth, h_f, was determined using the cross-section of case 1, see Table 1, as a reference. In Figure 3.39 the relative resistance curves are shown for three flange depth values: 40, 48 and 56 mm. From Figure 3.40 to 3.27 we can see that there is no effect on charring for bending resistances not exceeding 20 % of the ambient value.

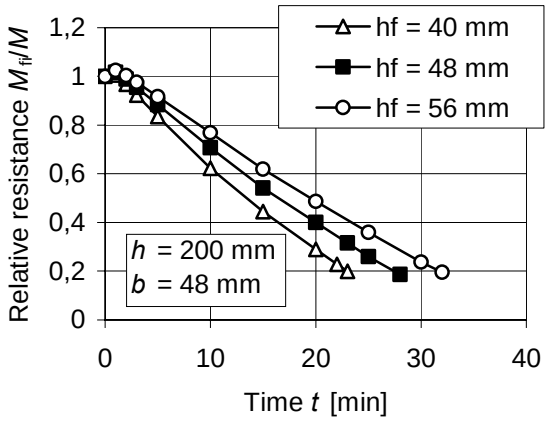

Figure 3.39 – Relative resistance vs. time – Effect of flange depth

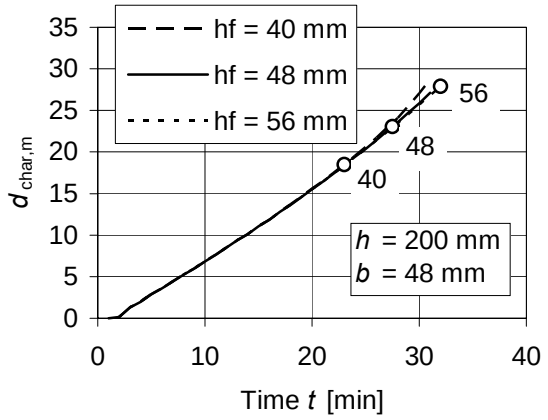

Figure 3.40 – Effect of flange depth on charring depth in the middle of the flange (the data points shown as circles are at times when the relative bending resistance is 0,2)

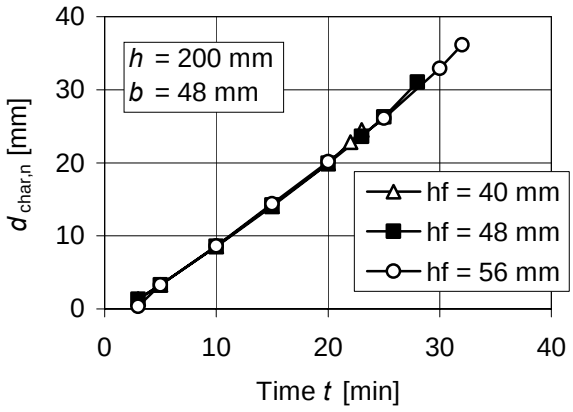

Figure 3.41 – Effect of flange depth on notional charring rate

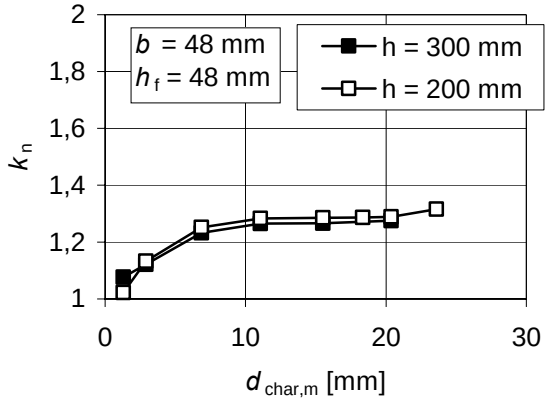

Figure 3.42 – Effect of flange depth on k_n

3.7.2 Modification factor for bending strength

Since there is no effect of flange depth on charring, the effect on the bending resistance shown in Figure 3.39 is solely related to the effect of the flange depth on the bending strength reduction, see Figure 3.43.

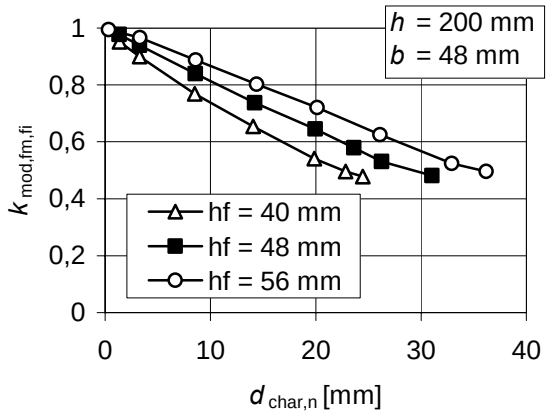

Figure 3.43 – Effect of flange depth on $k_{mod,fm,fi}$

In order to determine $k_{hf,fm}$ to be inserted in Equation (2.16), using the same procedure as in 3.6.2, a trend line was determined (Figure 3.44) as

$$k_{hf,fm} = 1,416 \times \frac{48}{h_f} - 0,4085 \tag{3.15}$$

and, after modification, as

$$k_{hf,fm} = \frac{68}{b} + 0,41 \tag{3.16}$$

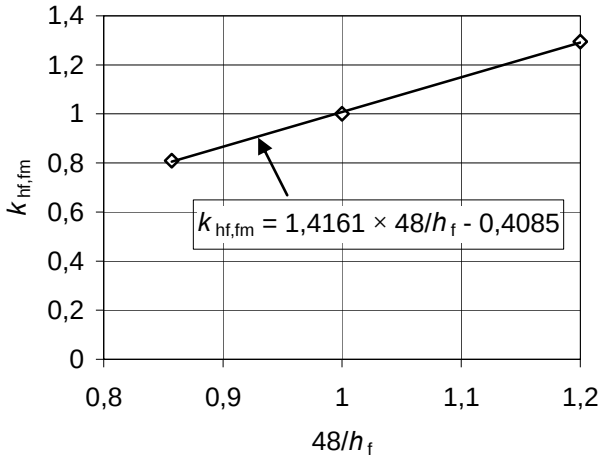

Figure 3.44 – Determination of effect of flange depth on bending strength

3.8 Effect of cross-section depth

3.8.1 Bending resistance and charring

In order to determine the effect of cross-section depth, the cross-section of case 1, however with h = 300 mm, was analyzed. Figure 3.45 shows that an increase of the depth by 50 % gives slightly smaller bending resistance, especially at load levels between 30 and 20 %. It is evident that there cannot be an influence on the charring depth in the middle of the flange; moreover, in Figure 3.46 and 3.37 no significant effect on the notional charring depth can be seen.

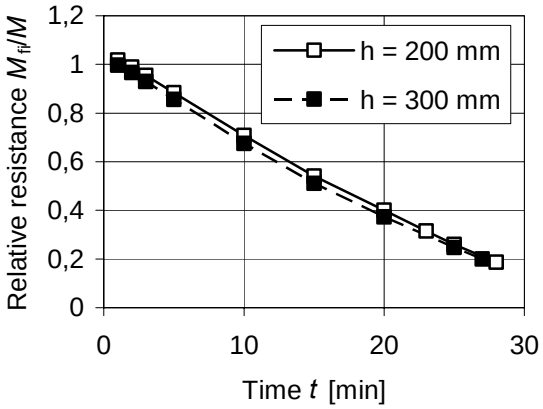

Figure 3.45 – Relative resistance vs. time – Effect of depth of cross-section

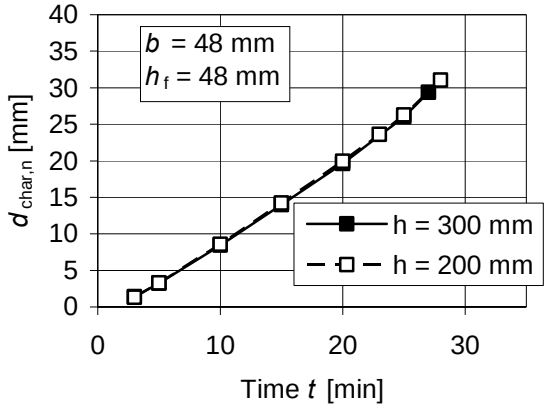

Figure 3.46 – Effect of cross-section depth on notional charring rate

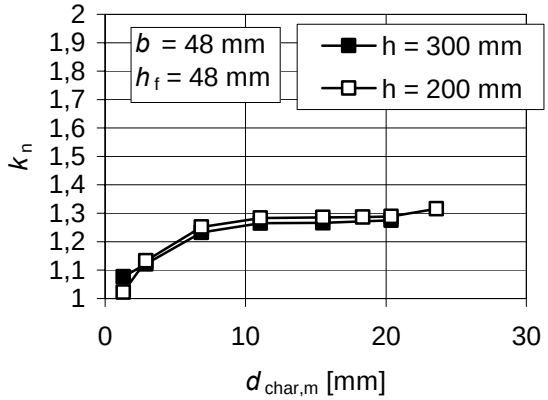

Figure 3.47 – Effect of cross-section depth on k_n

3.8.2 Modification factor for bending strength

Since the charring depth, both in the middle of the flange and the notional charring depth, are not affected by an increase of cross-section depth, the difference of bending resistance is solely caused by a slightly greater reduction of bending strength, see Figure 3.48, showing the relationships of the modification factor for bending strength vs. the notional charring depth. For a notional charring depth of 25 mm and a relative bending resistance of 0,25 the difference is about 5 %.

To determine $k_{h,fm}$ for inserting in Equation (2.17), using the same procedure as in 3.6.2, a linear relationship was determined (Figure 3.44) as:

$$k_{h,fm} = 1,404 - 0,404 \times \frac{200}{h} \tag{3.17}$$

and, after modification, as

$$k_{h,fm} = 1,4 - \frac{80}{h} \tag{3.18}$$

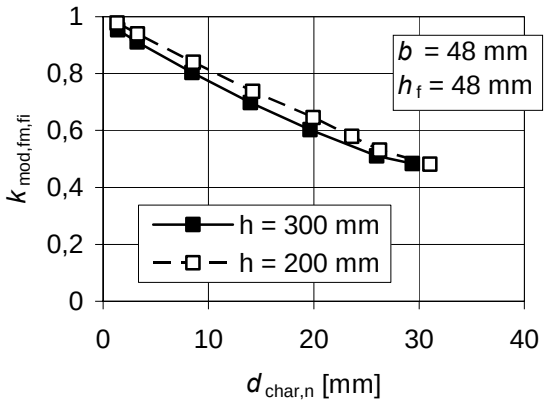

Figure 3.48 – Effect of cross-section depth on $k_{mod,fm,fi}$

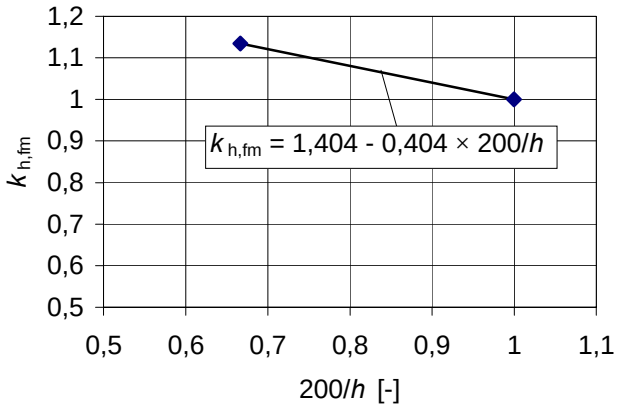

Figure 3.49 – Determination of depth effect on $k_{mod,fm,fi}$

3.9 Shear strength

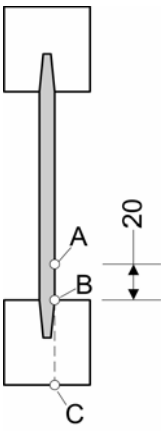

Figure 3.50 – Location of A, B and C

From Figure 3.7 can be seen that the maximum temperature in the web is reached at a distance of about 20 mm above the flange. Temperature histories at that location (location A in Figure 3.50) are shown in Figure 3.51 as functions of the normalized notional charring depth. For shear strength verification, the shear strength must be reduced. A modification factor of shear strength, $k_{mod,fv,fi}$, was calculated by multiplying the temperature by the reduction factor for shear strength given by EN 1995-1-2 [1] and shown in Figure 3.8, see Figure 3.52. A bi-linear model was fitted to the curves representing charring phase 3 as the most relevant scenario for floors in fire:

$$k_{\mathrm{mod,fv,fi}} = \begin{cases} 1 & \text{for} \quad \dfrac{48 k_{\mathrm{b,ch}}\, d_{\mathrm{char,n}}}{h_{\mathrm{f}}} \le 20 \\ 1,47 - \dfrac{1,13 k_{\mathrm{b,ch}}\, d_{\mathrm{char,n}}}{h_{\mathrm{f}}} & \text{for} \quad \dfrac{48 k_{\mathrm{b,ch}}\, d_{\mathrm{char,n}}}{h_{\mathrm{f}}} > 20 \end{cases} \tag{3.19}$$

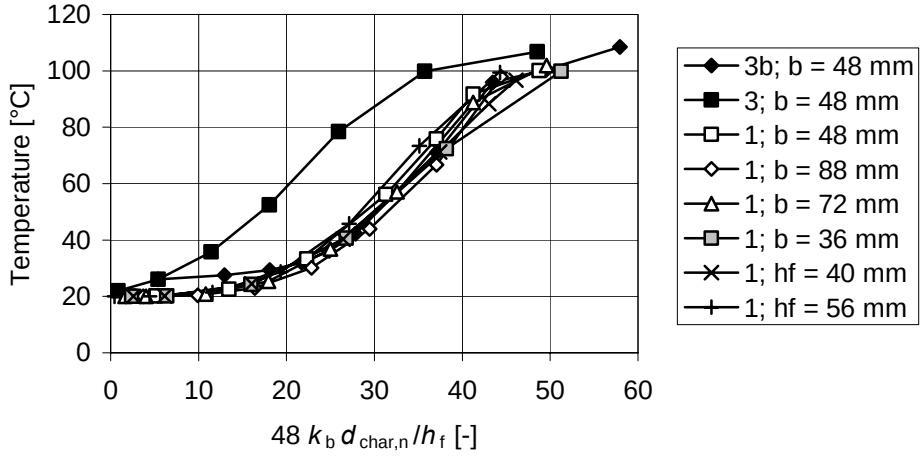

Figure 3.51 – Temperature development in the web 20 mm above the lower flange

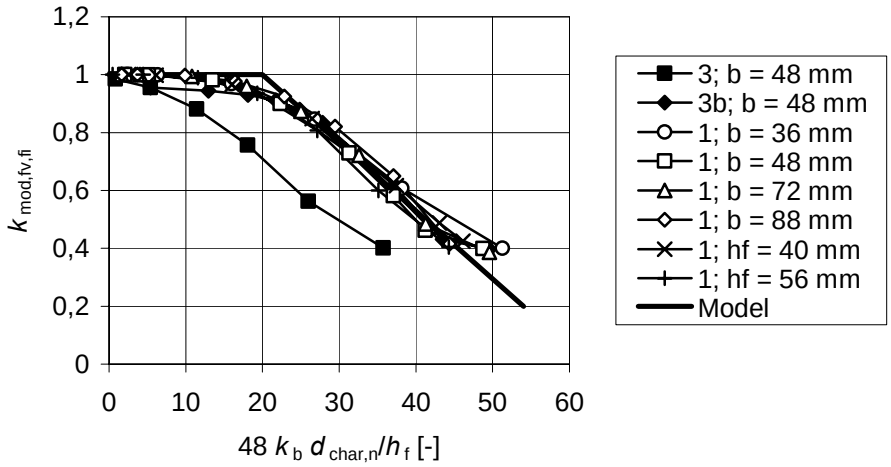

Figure 3.52 – Modification factor for shear strength

For shear strength verification of the glue-line between the web and the flange, the temperature profile along the line from B to C is relevant. For case 1 the profiles are shown in Figure 3.53 and the temperature development at B in Figure 3.54. The temperature profile is constant and does not exceed 100°C within a distance of 10 mm from B. Normally the bonded-in length of the web is between 15 and 20 mm. A simplified assumption of a bonded-in depth of 10 mm and the use of the temperature development in B, see Figure 3.54, would give conservative results of the shear resistance verification. A bi-linear model fitted to the temperature development at location B is given by:

$$\Theta_{\text{joint}} = \max \begin{cases} 666\, d_{\text{char,n}} \dfrac{k_{\text{b}}}{\sqrt{b}\; h_{\text{f}}} - 12 \\ 20 \end{cases} \tag{3.20}$$

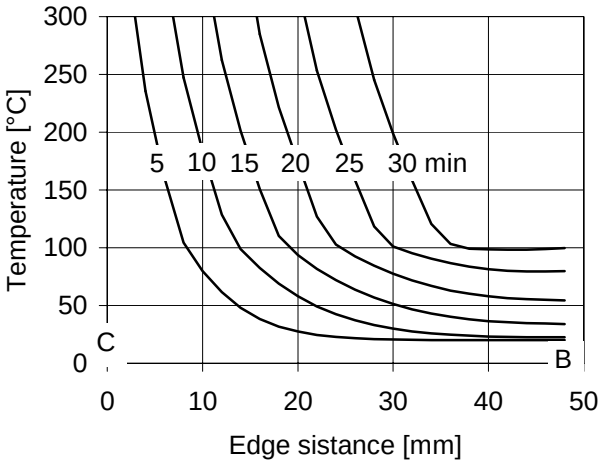

Figure 3.53 – Temperature profiles in the flange between B and C shown in Figure 3.50 for case 1

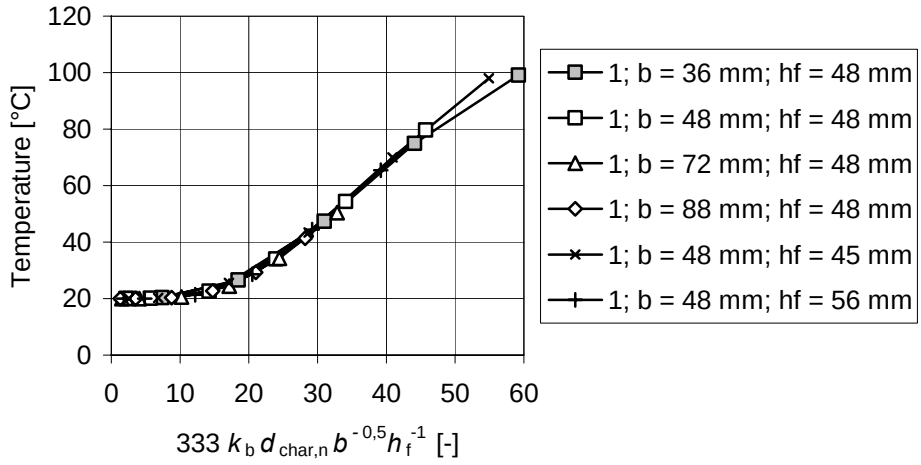

Figure 3.54 – Temperature development at location B (Figure 3.50)

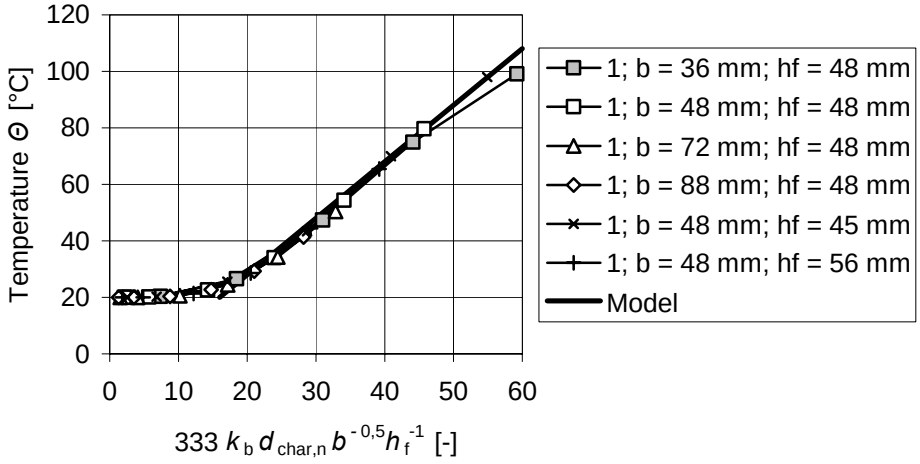

Figure 3.55 – Bi-linear model of temperature development at location B

4 Conclusions

In the previous sections, model parameters have been derived for a simple design model presented in section 2 for wooden I-joists in floor assemblies with cavities that completely filled with insulation. The model is valid for simply supported floors. Since no experimental verification is available to quantify the bending moment resistance at intermediate supports, floors with two or more spans should be assumed as a series of one-span floors. The model takes into account different charring phases with respect to protection provided by the cladding. For floor assemblies filled with glass wool insulation, the design model is considerably conservative for the period after failure of the cladding; we know from fire testing that there is a considerable period of time to failure of the floor even after the cladding has fallen off the floor. In this respect it will be possible to improve the model when thermal properties of glass fibre insulation become available that describe the degradation of the insulation above the melting point of the insulation.

5 References

[1] EN 1995-1-2:2004 Eurocode 5: Design of timber structures – Part 1-2: General – Structural fire design. European Standard. European Committee for Standardization, Brussels, 2004.

[2] Östman, B., König, J., Mikkola, E., Stenstad, V., Carlsson, J., and Karlsson, B., Brandsäkra trähus. Version 2. Trätek, Swedish Institute for Wood Technology Research, Publ. nr 0210034, Stockholm, 2002.

[3] König, J., Norén, J., Bolonius Olesen, F., Toft Hansen, F., Timber frame assemblies exposed to standard and parametric fires – Part 1: Fire tests. Trätek, Swedish Institute for Wood technology Research, Report I 9702015, Stockholm, 1997.

[4] Richardson, L. R., Thoughts and observations on fire-endurance tests of wood-frame assemblies protected by gypsum board. Proceedings of Wood and Fire, High Tatra, Slovakia, 2000.

[5] EN 1995-1-1:2004 Eurocode 5: Design of timber structures – Part 1-1: General – Common rules and rules for buildings. European Standard. European Committee for Standardization, Brussels, 2004.

[6] Franssen, J.M, Kodur, V.K.R., Mason, J., User's manual for SAFIR 2004 – A computer program for analysis of structures subjected to fire. University of Liege, Department Structures du Génie Civil – Service Ponts et Charpentes. Liege, Belgium, 2005.

[7] König, J. and Walleij, L., One-dimensional charring of timber exposed to standard and parametric fires in initially protected and non-protected fire situations. Trätek – Swedish Institute for Wood Technology Research, Report No. I 9908029, Stockholm, 1999.

[8] Sultan, M. A., A model for predicting heat transfer through noninsulated unloaded steel-stud gypsum board wall assemblies exposed to fire. Fire Techn., Third Quarter, 1996, 239-259.

[9] König, J. and Rydholm, D., Small-scale fire tests of heavy timber components. Trätek – Swedish Institute for Wood Technology Research, Report No. P 0310036, Stockholm, 2003.

[10] EN 520:2004, Gypsum plasterboards – Definitions, requirements and test methods. European Committee for Standardization, Brussels, 2004.

[11] Källsner, B. and König, J., Thermal and mechanical properties of timber and some other materials used in light timber frame construction. Proceedings of CIB W18, Meeting 33, Delft, Lehrstuhl für Ingenieurbau, University Karlsruhe, Karlsruhe, Germany, 2000.

[12] EN 338:2003, Structural timber – Strength classes. European Standard. European Committee for Standardization, Brussels, 2003.

[13] Thunell, B., Hållfasthetsegenskaper hos svenskt furuvirke utan kvistar och defekter. Royal Swedish Institute for Engineering Research, Proceedings No. 161, Stockholm, 1941

[14] EN 520:2004, Gypsum plasterboards – Definitions, requirements and test methods. European Committee for Standardization, Brussels, 2004.

[15] König, J., Fire resistance of timber joists and load bearing wall frames. Trätek – Swedish Institute for Wood Technology Research, Report No. I 9412071, Stockholm, 1995.

SP Swedish National Testing and Research Institute develops and transfers technology for improving competitiveness and quality in industry, and for safety, conservation of resources and good environment in society as a whole. With Swedens widest and most sophisticated range of equipment and expertise for technical investigation, measurement, testing and certfication, we perform research and development in close liaison with universities, institutes of technology and international partners.

SP is a EU-notified body and accredited test laboratory. Our headquarters are in Borås, in the west part of Sweden.

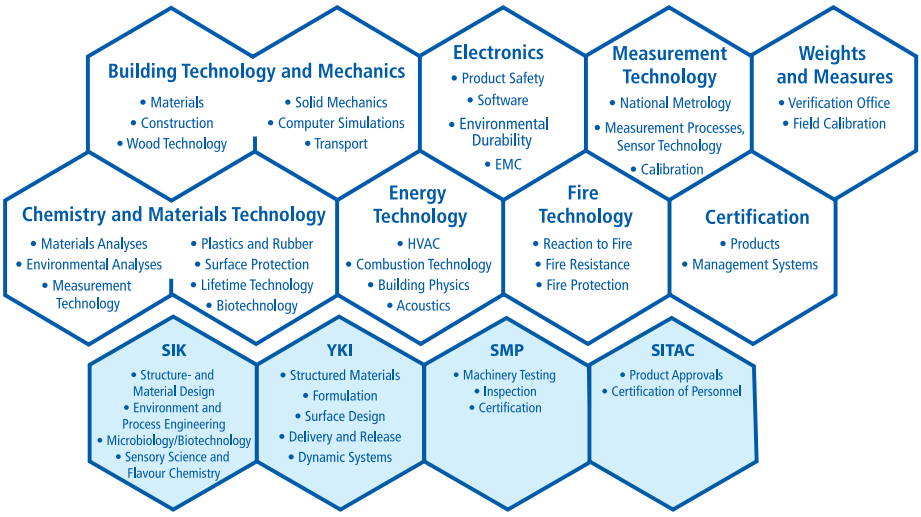

SP is organised into eight technology units and four subsidiaries

SP Wood Technology
SP REPORT 2006:44
ISBN 91-85533-32-7
ISSN 0284-5172

SP Swedish National Testing and Research Institute
Box 857
SE-501 15 BORÅS, SWEDEN
Telephone: + 46 33 16 50 00, Telefax: +46 33 13 55 02
E-mail: info@sp.se, Internet: www.sp.se